

Article

# A Graphic Method for Detecting Multiple Roots Based on Self-Maps of the Hopf Fibration and Nullity Tolerances

José Ignacio Extreminana-Aldana <sup>†‡</sup>, José Manuel Gutiérrez-Jiménez <sup>†‡</sup>, Luis Javier Hernández-Paricio <sup>\*,†‡</sup>  
and María Teresa Rivas-Rodríguez <sup>†‡</sup>

Department of Mathematics and Computer Science, University of La Rioja, 26006 Logroño, Spain; jextremi@unirioja.es (J.I.E.-A.); jmguti@unirioja.es (J.M.G.-J.); maria-teresa.rivas@unirioja.es (M.T.R.-R.)

\* Correspondence: luis-javier.hernandez@unirioja.es; Tel.: +34-941-299-468

† Current address: Departamento de Matemáticas y Computación, Edificio CCT—C/Madre de Dios, 53, 26006 Logroño, Spain.

‡ These authors contributed equally to this work.

**Abstract:** The aim of this paper is to study, from a topological and geometrical point of view, the iteration map obtained by the application of iterative methods (Newton or relaxed Newton's method) to a polynomial equation. In fact, we present a collection of algorithms that avoid the problem of overflows caused by denominators close to zero and the problem of indetermination which appears when simultaneously the numerator and denominator are equal to zero. This is solved by working with homogeneous coordinates and the iteration of self-maps of the Hopf fibration. As an application, our algorithms can be used to check the existence of multiple roots for polynomial equations as well as to give a graphical representation of the union of the basins of attraction of simple roots and the union of the basins of multiple roots. Finally, we would like to highlight that all the algorithms developed in this work have been implemented in Julia, a programming language with increasing use in the mathematical community.

**Keywords:** Newton's method; Hopf fibration; multiple roots; rational functions; homogeneous coordinates; Riemann sphere



**Citation:** Extreminana-Aldana, J.I.; Gutiérrez-Jiménez, J.M.; Hernández-Paricio, L.J.; Rivas-Rodríguez, M.T. A Graphic Method for Detecting Multiple Roots Based on Self-Maps of the Hopf Fibration and Nullity Tolerances. *Mathematics* **2021**, *9*, 1914. <https://doi.org/10.3390/math9161914>

Academic Editor: Anton Iliev

Received: 28 July 2021

Accepted: 9 August 2021

Published: 11 August 2021

**Publisher's Note:** MDPI stays neutral with regard to jurisdictional claims in published maps and institutional affiliations.



**Copyright:** © 2021 by the authors. Licensee MDPI, Basel, Switzerland. This article is an open access article distributed under the terms and conditions of the Creative Commons Attribution (CC BY) license (<https://creativecommons.org/licenses/by/4.0/>).

## 1. Introduction

In this paper, we present a geometrical and topological framework and some mathematical techniques to study a numerical method for solving nonlinear algebraic equations from a different point of view. In general, a root-finding method applied to a polynomial complex equation gives rise to rational functions that could be defined on the Riemann sphere. Instead of taking the iteration of a rational function on the Riemann sphere, we consider the iteration of a "function" on the Hopf fibration  $S^3 \rightarrow S^2 \cong \mathbf{P}^1(\mathbb{C})$ , where  $S^n$  denotes the  $n$ -sphere and  $\mathbf{P}^1(\mathbb{C})$  is the complex projective line. In addition, we develop a collection of algorithms for the iteration of a rational function that avoids the problem of overflows caused by denominators close to zero and the problem of indetermination which appears when simultaneously the numerator and denominator are equal to zero. Although these algorithms can be applied to any rational function, we focus our interest in rational functions that arise from the application of a numerical method for solving a nonlinear polynomial equation. In particular, we consider the relaxed Newton's method for solving polynomial equations, but our study could be generalized to other iterative methods. One of the main applications of our algorithms is the division of the Riemann sphere in three regions: the union of the basins of multiple roots, the union of the basins of simple roots, and the rest of the points. Consequently, our numerical procedures are appropriate for analyzing the existence of multiple roots of an equation.

It is interesting to observe that a rational map  $f(z) = \frac{p(z)}{q(z)}$  is given by a quotient of two polynomials  $p(z)$ ,  $q(z)$  and this representation can be or not be irreducible. In an iteration

process, on the one hand, you may encounter an overflow problem when  $p(z) \neq 0$  and  $q(z)$  is a very small complex number; on the other hand, if the representation of  $f(z)$  is not given in an irreducible expression, it can have common roots  $z_0$  of  $p(z) = 0$  and  $q(z) = 0$ . For  $z$  near  $z_0$ , an iteration algorithm has to compute  $p(z)$ ,  $q(z)$  and the quotient  $\frac{p(z)}{q(z)}$ . In these cases, you have an indeterminacy problem and the computer system cannot calculate the quotient  $\frac{p(z)}{q(z)}$ . As a consequence, the computational environment gives an error and the iteration process stops. We refer the reader to the penultimate section of [1] where this type of error is explained and some solutions are given through the technique of starting the iteration at a different point. Other useful methods based on the infinite-precision arithmetic [2,3] are able to avoid in many cases the types of errors that appear in the iteration process, but this technology is not a panacea. In this paper, we use the iteration of self-maps of the Hopf fibration and the use of normalization methods to avoid errors caused by overflow and indeterminacy problems.

In previous works ([4–6]), we have developed some homogeneous versions of numerical methods associated with a complex rational map  $a(z)/b(z)$ , where  $a, b$  are elements in the complex polynomial ring  $\mathbb{C}[z]$  and  $b \neq 0$ . The procedure used in these papers consists of changing  $a(z)/b(z)$  by  $F(u, v)/G(u, v)$ , where  $z = u/v$  and  $F(u, v), G(u, v)$  are homogeneous bivariate polynomials with the same degree; that is,  $R = (F, G)$  is a homogeneous pair (see current Definitions 2 and 3).

However, the present work is based on the iteration of a self-map of the pointed Hopf fibration: Given a homogeneous pair  $R = (F, G)$ , we consider the following commutative diagram:

$$\begin{array}{ccc}
 \mathbb{C}^2 & \xrightarrow{R} & \mathbb{C}^2 \\
 p \downarrow & & \downarrow p \\
 S^{3+} & \xrightarrow{R^S} & S^{3+} \\
 q \downarrow & & \downarrow q \\
 \mathbf{P}^{1+}(\mathbb{C}) & \xrightarrow{R^P} & \mathbf{P}^{1+}(\mathbb{C})
 \end{array}$$

where the pointed Hopf fibration  $q: S^{3+} \rightarrow \mathbf{P}^{1+}(\mathbb{C})$  is the canonical extension by an additional point of the well-known Hopf fibration  $q: S^3 \rightarrow \mathbf{P}^1(\mathbb{C})$ , see [7]. The definitions of  $p: \mathbb{C}^2 \rightarrow S^{3+}$  and  $q: S^{3+} \rightarrow \mathbf{P}^{1+}(\mathbb{C})$  are given by Formula (4) in Section 2.2. The definitions of  $R, R^S, R^P$  appear in (9)–(11), respectively.

In a first approach, we are interested in solving a nonlinear equation  $g(z) = 0$ , where  $g: \mathbb{C} \rightarrow \mathbb{C}$  is a  $d$ -degree polynomial, by using the well-known relaxed Newton’s method

$$z_{n+1} = N_\mu(g)(z_n) = \frac{z_n g'(z_n) - \mu g(z_n)}{g'(z_n)}, \quad n \geq 0, \quad \mu \in \mathbb{C}. \tag{1}$$

Note that the classical Newton’s method is obtained for  $\mu = 1$ . If the previous sequence starts at an initial approximation  $z_0$  close enough to a root of the polynomial  $g$ , then it converges to such a root. The influence of the multiplicities of the roots of the polynomial  $g$  in the numerical and dynamical properties of a rootfinding method has been analyzed by several authors, see [5,6,8–10]. In addition, the importance of the relaxing parameter  $\mu$  in the convergence of the sequence defined in (1) has been studied in papers like [11] or [12], for instance.

In this work, from a theoretical point of view, we consider the Newton and relaxed Newton methods as endomorphisms of the pointed Hopf fibration. That is, the relaxed

Newton method associated with a complex polynomial  $g \in \mathbb{C}[z]$  is given by a homogeneous pair  $R = (F, G)$  such that the following induced diagram is commutative:

$$\begin{CD} S^{3+} @>R^S=[F,G]>> S^{3+} \\ @VqVV @VVqV \\ \mathbf{P}^{1+}(\mathbb{C}) @>R^P=[F:G]>> \mathbf{P}^{1+}(\mathbb{C}). \end{CD}$$

Moreover, if  $(F, G) \neq (0, 0)$  is irreducible (see Definition 5), one has that  $R^S(S^3) \subset S^3$  and  $R^P(\mathbf{P}^1(\mathbb{C})) \subset \mathbf{P}^1(\mathbb{C})$ ; therefore, the restriction in the diagram above to  $S^3 \rightarrow \mathbf{P}^1(\mathbb{C})$  is an endomorphism of the standard Hopf fibration.

The augmented complex projective line  $\mathbf{P}^{1+}(\mathbb{C}) = \mathbf{P}^1(\mathbb{C}) \cup \{\bar{0}\}$  is obtained by adding a new point  $\bar{0}$  to the usual complex projective line  $\mathbf{P}^1(\mathbb{C})$ . In this paper, when  $R \neq (0, 0)$ , we analyze the properties of the finite set of proper indeterminate points  $\text{PInd}(R^P) = \mathbf{P}^1(\mathbb{C}) \cap (R^P)^{-1}(\{\bar{0}\})$ . If we remove the indetermination points of a homogeneous pair  $R$  (that is, we eliminate the common zeros of the numerator and denominator of a rational map presented as a quotient of polynomials), we obtain a new irreducible homogeneous map which is denoted by  $\text{red}(R)^P$ . The set  $\text{PInd}(R^P)$  has the following properties:

- If  $\text{PInd}(R^P) = \emptyset$ , then  $R = (F, G)$  is irreducible, the restriction of the pair  $(R^S, R^P)$  is an endomorphism of the Hopf fibration  $q: S^3 \rightarrow \mathbf{P}^1(\mathbb{C})$ , and  $R^P: \mathbf{P}^1(\mathbb{C}) \rightarrow \mathbf{P}^1(\mathbb{C})$  is an analytic global map of the Riemann sphere ( $\mathbf{P}^1(\mathbb{C}) \cong S^2 \cong \hat{\mathbb{C}}$ .)
- If  $\text{PInd}(R^P) \neq \emptyset$ , then  $R = (F, G)$  is not irreducible and the proper basin of  $\bar{0}$  is contained in the union of the basins of end points associated with proper indeterminate points of  $R^P$  in  $\mathbf{P}^1(\mathbb{C})$  taking as iteration map  $\text{red}(R)^P: \mathbf{P}^1(\mathbb{C}) \rightarrow \mathbf{P}^1(\mathbb{C})$ , where  $\text{red}(R)^P$  is the irreducible pair obtained from  $R$  by a canonical procedure (see (15)).

The algorithms associated with the iteration of the self-map  $R^P: \mathbf{P}^{1+}(\mathbb{C}) \rightarrow \mathbf{P}^{1+}(\mathbb{C})$  have the difficulty of the choice of a suitable representative element in the equivalence class  $[z : t] = \{\lambda(z, t) \in \mathbb{C}^2 \mid \lambda \in \mathbb{C} \setminus \{0\}\}$ . Since  $\mathbf{P}^{1+}(\mathbb{C})$  is a quotient of  $S^{3+}$  and  $S^{3+}$  is a quotient of  $\mathbb{C}^2$ , we have tackled this problem using the iteration of the self- map  $(R, R^S)$  given in the commutative diagram:

$$\begin{CD} \mathbb{C}^2 @>R>> \mathbb{C}^2 \\ @VpVV @VVpV \\ S^{3+} @>R^S>> S^{3+}, \end{CD}$$

and the fact that Equations (2)–(4), (7), (8), (12) and (14)–(16) are formulated in terms of usual computational types (integers, real and complex numbers, arrays, etc.) that can be easily implemented in many computational languages. In this case, we have implemented these formulas and associated algorithms in Julia Language (in some previous papers, we have developed other algorithms and implementations in Mathematica and Sage [13,14]).

In this work, we focus on the development of the theory of the iteration of endomorphisms (of type  $(R, R^S)$ ) of the pointed Hopf fibration and the design of algorithms for the study of indeterminate points (for a detailed description of the implementation of these algorithms in Julia, we refer the reader to [15].)

The Julia programming language has very nice properties: It has automatic translation of formulas into efficient executable code. It allows programmers to write clear, high-level, generic, and abstract code that closely resembles mathematical formulas, as they have grown accustomed to in dynamical systems, yet produces fast, low-level machine code that has traditionally only been generated by static languages. Moreover, one can easily use parallel programming to obtain faster computational executions. For more complete information, we refer the reader to the paper [16] by Bezanson, Edelman, Karpinski, and Shah who started working on Julia language in 2009.

One of the objectives of this work is the construction of algorithms to detect the existence of multiple roots of polynomial equations. These algorithms are designed to have a high performance and can be easily implemented in programming languages like Julia. Its design is based on the evaluation of a canonical function associated with a homogeneous pair in the orbit of a point in the Riemann sphere (see Section 4). To do this, instead of working with the complex rational functions that arise from methods (1), we consider the homogeneous version of the methods (see Section 5.1).

For the relaxed Newton method, the existence of proper indeterminate points is equivalent to the existence of multiple roots (see Theorem 2). In addition, the use of homogeneous coordinates and the inclusion of new points in our model (the infinity point, a super-zero point) has a series of numerical advantages, avoiding overflows and underflows in the calculations.

In order to obtain a graphic representation of the union of the basins of attraction of the multiple roots and the union of the basins of attraction of the simple roots, we divide the complex projective line into three disjoint regions

$$\mathbf{P}^1(\mathbb{C}) = \text{Red} \cup \text{Green} \cup \text{Black}.$$

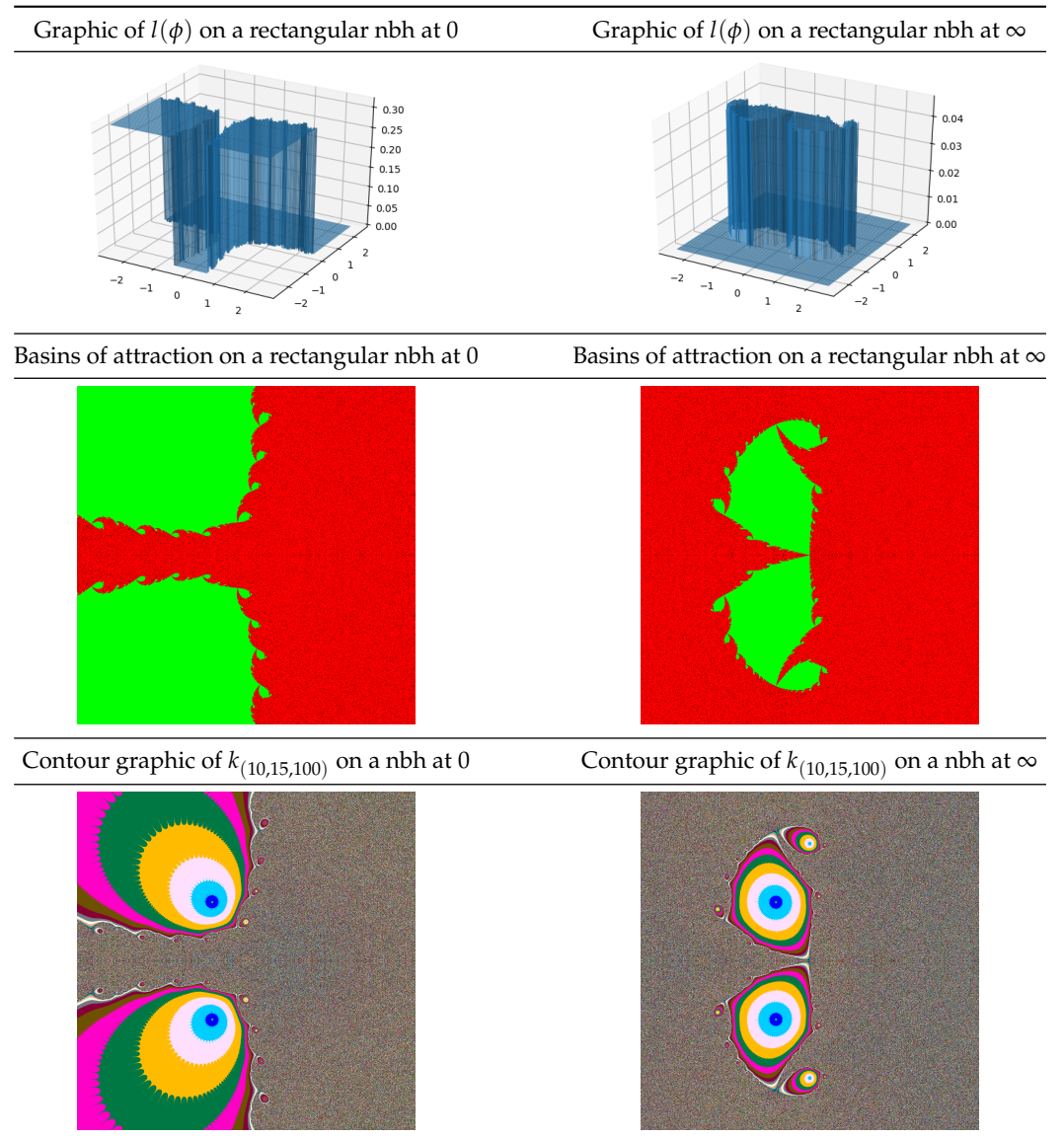
The red region Red is the union of the proper basins of end points associated with proper indeterminate points  $\text{PInd}(R^P)$  under the iteration of  $\text{red}(R)^P$ , see Section 2.1. Note that Red contains the proper basin (under the iteration of  $R^P$ ) of the super-zero point  $\bar{0}$ . The green region Green is the union of the basins of fixed points which are not proper indeterminate points, and Black is the complementary subset:  $\text{Black} = \mathbf{P}^1(\mathbb{C}) \setminus (\text{Red} \cup \text{Green})$ .

In this work, we have developed algorithms implemented in Julia language which give a graphical approach to these three regions, see Tables 1 and 2. For given tolerances  $10^{-N}$ ,  $10^{-C}$ , where  $N, C \in \mathbb{N}$ , the implemented algorithms give pixelated regions  $\text{Red}_{(N,C)}$ ,  $\text{Green}_{(N,C)}$ ,  $\text{Black}_{(N,C)}$  approaching the regions Red, Green, Black.

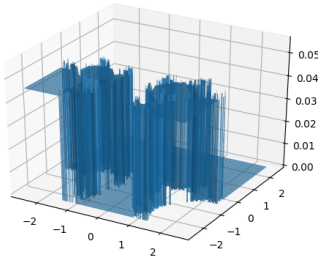
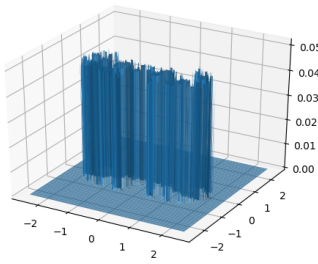
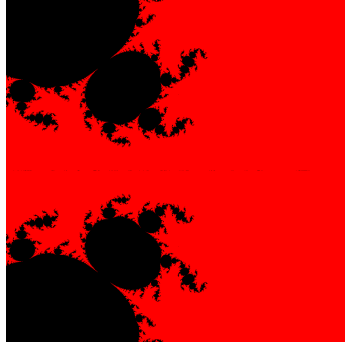
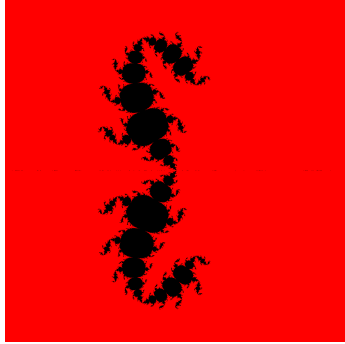
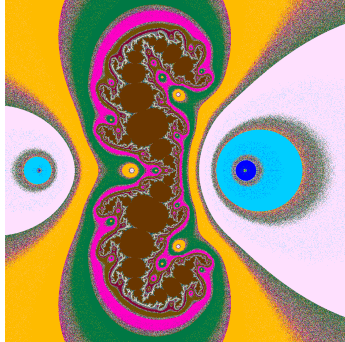
In particular, we study homogeneous pairs obtained by applying the Homogeneous relaxed Newton method  $R = \text{HN}_\mu(g)$  to a univariate complex polynomial  $g$ . For the relaxed method, by Theorem 2, we have that  $\text{MZ}(g) \cong \text{PInd}(\text{HN}_\mu(g)^P)$ ; that is, there is a bijective correspondence between the finite set of multiple roots of  $g$  and the finite set of proper indeterminate points of  $\text{HN}_\mu(g)^P$ . In this case, one has that the region Red is the union of the basins of multiple roots and the region Green is the union of the basins of simple roots. Therefore, when one obtains a non-empty red region, the polynomial  $g$  has at least a multiple root. However, we have to take into account that, in a computational environment, we usually work modulo some tolerances; therefore, in some cases, a red region in a graphical representation could be a consequence of the existence of a cluster of simple roots contained in a very small disk. For more results about the relations between clusters of simple roots and multiple roots, we refer the reader to [17].

We remark that our approach considers a numerical method as a self-map of the pointed Hopf fibration which is closely related to the self-maps on the Riemann sphere. There is much literature about the iteration of a rational map on the Riemann Sphere; for more information, we refer the reader to [18–20].

**Table 1.** (Relaxation parameter  $\mu = 1$ ) The first row gives a graphic of the function  $l(\phi)$  associated with  $HN(p)$  in a neighborhood (nbh) at the origin and at the infinity point, respectively. In the second row, we have a global representation of the union of basins of multiple roots in red and the union of basins of simple roots in green. In the third row, we use different colors to give a contour graphic of the function  $k_{(10,15,100)}$ .



**Table 2.** (Relaxation parameter  $\mu = 2$ ) The first row gives a graphic of the function  $l(\phi)$  associated  $HN_2(p)$  in a neighborhood (nbh) at the origin and at the infinity point, respectively. In the second row, we have a global representation of the union of basins of multiple roots in red. In the third row, we use different colors to give a contour graphic of the function  $k_{(10,15,100)}$ .

|   |   |
|---|---|
| Graphic of $l(\phi)$ on a rectangular nbh at 0                                      | Graphic of $l(\phi)$ on a rectangular nbh at $\infty$                                 |
|    |    |
| Basins of attraction on a rectangular nbh at 0                                      | Basins of attraction on a rectangular nbh at $\infty$                                 |
|   |   |
| Contour graphic of $k_{(10,15,100)}$ on a nbh at 0                                  | Contour graphic of $k_{(10,15,100)}$ on a nbh at $\infty$                             |
|  |  |

## 2. Preliminaries

In order to create a theoretical basis to hold and justify the correct construction of our algorithms for the representation of basins of end points corresponding to rational maps, we shall use the mathematical techniques described in this section. This study will be developed within the theoretical framework of dynamics on the Hopf fibration which is related to the complex dynamics on the Riemann sphere and dynamics on the 3-sphere.

### 2.1. Discrete Metric Semi-Flows and Basins

If  $X$  is a metric space with metric  $d$  and  $h: X \rightarrow X$  is a continuous map, then  $(X, h)$  is said to be a *metric discrete semi-flow* that will shortly be denoted by  $X$ . Given an integer  $n \geq 0$ ,  $h^n$  denotes the  $n$ -th composition  $h \circ \dots \circ h$  and  $h^0 = id_X$ . We consider the usual notions of *fixed point*, *periodic point* and  *$q$ -cyclic point* of  $h$ . Note that  $x \in X$  is a  $q$ -periodic point if and only if  $x$  is a fixed point of  $h^q$ .

The end space of  $X$  is the quotient:  $\Pi(X) = \frac{\{(h^n(x))_{n \in \mathbb{N}} | x \in X\}}{\sim}$ , where, for  $x, y \in X$ ,  $(h^n(x)) \sim (h^n(y))$  if and only if  $(d(h^n(x), h^n(y))) \xrightarrow{n \rightarrow +\infty} 0$ . An element  $a = [(h^n(x))] \in \Pi(X)$  is called an *end point* of  $X$ . Note that any point  $x \in X$  induces an end point represented by  $(h^n(x))$ . Therefore, one has a natural map  $\omega: X \rightarrow \Pi(X)$ ,  $\omega(x) = [(h^n(x))] = [(x, h(x), h^2(x), \dots)]$ . In particular, a fixed point  $x$  determines an end point represented by the constant sequence  $(x)$ .

The map  $\omega$  decomposes the discrete semi-flow  $X = \sqcup_{a \in \Pi(X)} B(a)$ , where  $B(a) = \omega^{-1}(a)$ ,  $a \in \Pi(X)$ , is said to be the *basin of the end point*  $a$ . In particular, if  $x_0 \in X$  is a fixed point, we have that the basin of  $x_0$  is given by  $\omega^{-1}([(x_0, x_0, \dots)])$ .

Here, we also consider the case of augmented metric spaces of the form  $X^+ = X \cup \{*\}$  ( $* \notin X$ ) which are provided with a metric  $d$  extending the metric  $d$  of  $X$ . We analyze the iteration of a continuous map  $f: X^+ \rightarrow X^+$  with the additional property that  $f(*) = *$ . In this work, the construction  $X^+$  will be used for  $X = S^2 \subset \mathbb{R}^3$  taking  $* = (0, 0, 0) \in \mathbb{R}^3$ ,  $X = S^3 \subset \mathbb{C}^2$  taking  $* = (0, 0) \in \mathbb{C}^2$  and for  $X = \mathbf{P}^1(\mathbb{C})$  taking  $* = [0 : 0]$ , see Section 2.2. In these examples, since the additional point is induced by different tuples with 0's, we will use the notation  $* = \bar{0}$ .

**Definition 1.** Given a map  $f: X^+ \rightarrow X^+$ , a point  $x \in X^+$  is said to be a fixed point if  $f(x) = x$  and  $x$  is said to be a proper fixed point if  $x$  is a fixed point and  $x \neq *$ . Denote by  $\text{Fix}(f)$ ,  $\text{PFix}(f)$  the subsets of fixed points and proper fixed points of  $f$ , respectively. A point  $x \in X^+$  is said to be an indeterminate point if  $f(x) = *$  and  $x$  is said to be a proper indeterminate point if  $x$  is an indeterminate point and  $x \neq *$ . Denote by  $\text{Ind}(f)$ ,  $\text{PInd}(f)$  the subsets of indeterminate points and proper indeterminate points of  $f$ , respectively.

In these cases, the map  $\omega$  decomposes the discrete semi-flow  $X^+$  as a disjoint union of basins. If  $B$  is a basin of  $f$ , we say that the intersection  $B \cap X$  is a *proper basin* of  $f: X^+ \rightarrow X^+$ . Notice that if  $\{*\}$  is invariant by  $f$ ; that is,  $f^{-1}(\{*\}) = \{*\}$ , then  $\text{PInd}(f) = \emptyset$  and  $f(X) \subset X$ . If in the context this is clear, the restriction  $f|_X: X \rightarrow X$  is also denoted by  $f$ .

### 2.2. The Augmented Sphere and the Augmented Complex Projective Line

With the aim of studying the iteration of a complex rational map, we will use the following models and isomorphisms:  $S^2 = \{(r_1, r_2, r_3) \in \mathbb{R}^3 \mid r_1^2 + r_2^2 + r_3^2 = 1\}$  is the unit 2-sphere,  $\hat{\mathbb{C}} = \mathbb{C} \cup \{\infty\}$  denotes the Alexandroff compactification of  $\mathbb{C}$  and  $\mathbf{P}^1(\mathbb{C})$  denotes the complex projective line given by  $\mathbf{P}^1(\mathbb{C}) = \mathbb{C}^2 \setminus \{(0, 0)\} / \sim$ , where  $(z, t) \sim (z', t')$  if there exists a  $\lambda \in \mathbb{C} \setminus \{0\}$  such that  $(z, t) = (\lambda z', \lambda t')$  (the equivalence class of  $(z, t)$  is denoted by  $[z : t]$ ).

We have the isomorphisms  $\tilde{\theta}: S^2 \rightarrow \hat{\mathbb{C}}, \theta: \mathbf{P}^1(\mathbb{C}) \rightarrow \hat{\mathbb{C}}$ :

$$\tilde{\theta}(r_1, r_2, r_3) = \begin{cases} \frac{r_1}{1-r_3} + i \frac{r_2}{1-r_3}, & \text{if } r_3 < 1, \\ \infty, & \text{if } r_3 = 1. \end{cases} ; \quad \theta([z : t]) = \begin{cases} z/t, & \text{if } t \neq 0, \\ \infty, & \text{if } t = 0, \end{cases}$$

and the induced isomorphism  $\tilde{\theta}^{-1}\theta: \mathbf{P}^1(\mathbb{C}) \rightarrow S^2$ .

We also consider the *augmented 2-sphere*  $S^{2+} = S^2 \sqcup \{(0, 0, 0)\}$  and the *augmented complex projective line*  $\mathbf{P}^{1+}(\mathbb{C})$ , given by  $\mathbf{P}^{1+}(\mathbb{C}) = \mathbb{C}^2 / \sim$ , where  $(z, t) \sim (z', t')$  if there exists a  $\lambda \in \mathbb{C} \setminus \{0\}$  such that  $(z, t) = (\lambda z', \lambda t')$  (the equivalence class of  $(z, t)$  is also denoted by  $[z : t]$ .) Note that we have a canonical isomorphism  $\mathbf{P}^{1+}(\mathbb{C}) \cong \mathbf{P}^1(\mathbb{C}) \sqcup \{[0 : 0]\}$ , where one can reduce the notation using  $\bar{0} = [0 : 0]$ .

We also have the extended isomorphism  $(\tilde{\theta}^{-1}\theta)^+: \mathbf{P}^{1+}(\mathbb{C}) \rightarrow S^{2+}$  given by

$$(\tilde{\theta}^{-1}\theta)^+([z : t]) = \begin{cases} (0, 0, 0) & \text{if } \bar{t}t + z\bar{z} = 0, \\ \left( \frac{z\bar{t} + z\bar{t}}{\bar{t}t + z\bar{z}}, \frac{i(\bar{z}t - z\bar{t})}{\bar{t}t + z\bar{z}}, \frac{-\bar{t}t + z\bar{z}}{\bar{t}t + z\bar{z}} \right) & \text{in other cases.} \end{cases} \tag{2}$$

Since  $S^{2+}$  is a subspace of  $\mathbb{R}^3$ , the usual Euclidean metric of  $\mathbb{R}^3$  induces a Euclidean chordal metric  $d$  on  $S^{2+}$ . Using the bijection  $(\tilde{\theta}^{-1}\theta)^+ : \mathbf{P}^{1+}(\mathbb{C}) \rightarrow S^{2+}$ , we can translate the metric structure from  $S^{2+}$  to  $\mathbf{P}^{1+}(\mathbb{C})$  with the following formula:

$$d([z : t], [z' : t']) = d((\tilde{\theta}^{-1}\theta)^+([z : t]), (\tilde{\theta}^{-1}\theta)^+([z' : t'])), \tag{3}$$

where we have denoted again by  $d$  the induced metric on  $\mathbf{P}^{1+}(\mathbb{C})$ .

In this paper, we also consider the subspace  $S^3 = \{(z, t) \in \mathbb{C}^2 \mid |z| + |t| = 1\}$  of  $\mathbb{C}^2$ , where  $|\lambda|$  represents the absolute value (or modulus) of a complex number  $\lambda$ , and its augmented version  $S^{3+} = S^3 \cup \{(0, 0)\}$ . We are going to work with the composite of quotients:

$$\mathbb{C}^2 \rightarrow S^{3+} \rightarrow \mathbf{P}^{1+}(\mathbb{C})$$

given by the following relations:

Let  $(z, t), (z', t')$  be in  $\mathbb{C}^2$ :  $(z, t) \sim_p (z', t')$  if there is  $\lambda \in \mathbb{R}, \lambda > 0$ , such that  $(z', t') = \lambda(z, t)$ .

Let  $(z, t), (z', t')$  be in  $S^{3+}$ :  $(z, t) \sim_q (z', t')$  if there is  $\lambda \in \mathbb{C}, |\lambda| = 1$ , such that  $(z', t') = \lambda(z, t)$ .

These equivalence relations induce the following quotient maps:

$$p : \mathbb{C}^2 \rightarrow S^{3+}, \quad p((z, t)) = [z, t], \quad (z, t) \in \mathbb{C}^2$$

$$[z, t] = \begin{cases} (0, 0) & \text{if } |z| + |t| = 0, \\ \left(\frac{z}{|z|+|t|}, \frac{t}{|z|+|t|}\right) & \text{in other cases.} \end{cases} \tag{4}$$

$$q : S^{3+} \rightarrow \mathbf{P}^{1+}(\mathbb{C}), \quad q((z, t)) = [z : t], \quad (z, t) \in S^{3+}.$$

Given a point  $[z : t] \in \mathbf{P}^1(\mathbb{C})$ , a representative pair  $(z, t)$  is called the *homogeneous coordinates* of this point and, in this work, we call *normalized homogeneous coordinates* to the pair  $[z, t] = \left(\frac{z}{|z|+|t|}, \frac{t}{|z|+|t|}\right)$ . Given a pair  $(z, t) \in \mathbb{C}^2$ , its normalization  $[z, t]$  is defined by Formula (4).

We note that the chordal metric given on  $\mathbf{P}^{1+}(\mathbb{C})$  induces chordal pseudo-metrics on  $S^{3+}$  and  $\mathbb{C}^2$  by the formulas:

$$d((z_1, t_1), (z_2, t_2)) = d([z_1 : t_1], [z_2 : t_2]), \quad (z_1, t_1), (z_2, t_2) \in S^{3+} \tag{5}$$

$$d((z_1, t_1), (z_2, t_2)) = d([z_1, t_1], [z_2, t_2]), \quad (z_1, t_1), (z_2, t_2) \in \mathbb{C}^2. \tag{6}$$

Observe that, if we are working in a computational environment with a prefixed *Nullity Tolerance*  $10^{-N}$ ,  $N \in \mathbb{N}$ , and we have a point  $[z : t] \in \mathbf{P}^1(\mathbb{C})$  whose homogeneous coordinates  $(z, t)$  verify that  $|z| + |t| \leq 10^{-N}$ , then the computation system can take  $(z, t)$  as  $(0, 0)$ . This is the reason why we consider the space  $\mathbf{P}^{1+}(\mathbb{C}) = \mathbf{P}^1(\mathbb{C}) \cup \{[0 : 0]\}$  and the quotient map  $p_N : \mathbb{C}^2 \rightarrow S^{3+}$ , given by

$$p_N((z, t)) = [z, t]_N = \begin{cases} (0, 0) & \text{if } |z| + |t| \leq 10^{-N}, \\ \left(\frac{z}{|z|+|t|}, \frac{t}{|z|+|t|}\right) & \text{in other cases,} \end{cases} \tag{7}$$

and the composite  $qp_N : \mathbb{C}^2 \rightarrow S^{3+} \rightarrow \mathbf{P}^{1+}(\mathbb{C})$ . Notice that  $\lim_{N \rightarrow +\infty} p_N = p$ .

**Remark 1.** *The homogeneous coordinates have the property that a pair (tuple) and its normalization represent the same point in  $\mathbf{P}^1(\mathbb{C})$ . We can normalize homogeneous coordinates with the function given in (4). However, in order to obtain an implementation in Julia, it is better to work with normalized coordinates modulo some nullity tolerance ( $10^{-N}$ ) using the Formula (7). To see all the details of the implementations of Formulas (2) and (4)–(7), we refer the reader to [15].*

We remark that the use of the normalized homogeneous coordinates presented in this subsection allow us to represent the infinity point in  $\hat{\mathbb{C}}$  and to avoid overflow and underflow errors and indeterminacies in our computer programs.

### 3. Homogeneous Pairs

#### 3.1. Homogeneous Pairs of Complex Rational Maps

Let  $\mathbb{C}[z]$  be the ring of polynomials with complex coefficients and  $\mathbb{C}(z)$  the field of complex rational functions  $f(z) = \frac{A(z)}{B(z)}$  where  $A, B \in \mathbb{C}[z]$ , and  $B$  is not the zero polynomial. The degree  $d$  of  $f$  is given by  $d = \max\{\text{degree}(A), \text{degree}(B)\}$ , where the degree of the zero polynomial is taken to be  $-\infty$ .

Let  $\mathbb{C}[z, t]$  be the ring of bivariate polynomials with complex coefficients.

**Definition 2.** Given  $F \in \mathbb{C}[z, t]$ , it is said to be a homogeneous bivariate polynomial if  $F = 0$  or there is  $k \in \mathbb{N}$  such that, for every  $\lambda \in \mathbb{C} \setminus \{0\}$ ,  $F(\lambda z, \lambda t) = \lambda^k F(z, t)$  for every  $z, t \in \mathbb{C}$ . If  $F \neq 0$  is a homogeneous bivariate polynomial, it is said that the integer  $k$  is the degree of  $F$ .

Denote by  $\mathbb{C}_h[z, t]$  the subset of homogeneous bivariate polynomials.

A homogeneous bivariate polynomial  $F$  with degree  $k \geq 0$  can be expressed as  $F(z, t) = \sum_{i=0}^k a_i z^i t^{k-i}$ ,  $a_i \in \mathbb{C}$ , and, if  $n = \min\{m \mid a_i = 0 \text{ for } i \geq m\}$ , one has that  $a_n \neq 0$ , and we will write  $F$  as  $F(z, t) = \sum_{i=0}^n a_i z^i t^{k-i}$ ,  $a_i \in \mathbb{C}$ ,  $a_n \neq 0$ ,  $n \leq k$ .

If  $\mathbb{C}[x] \times \mathbb{N} = \{(A, d) \in \mathbb{C}[x] \times \mathbb{N} \mid \text{degree}(A) \leq d\}$ , we can consider the following homogenization operator:

$$H(A, d) = \begin{cases} 0 & \text{if } A = 0, \\ a_0 t^d + a_1 z t^{d-1} + \dots + a_n z^n t^{d-n} & \text{if } A \neq 0, A = a_0 + a_1 x + \dots + a_n x^n, a_n \neq 0, \end{cases} \tag{8}$$

Note that, if  $A \neq 0$ ,  $H(A, d)(\lambda z, \lambda t) = \lambda^d H(A, d)(z, t)$ .

**Definition 3.** Given  $F, G \in \mathbb{C}_h[z, t]$ , the pair  $(F, G)$  is said to be a homogeneous pair if either the product  $FG = 0$  or  $F$  and  $G$  have the same degree. We say that  $d = \max\{\text{degree}(F), \text{degree}(G)\}$  is the degree of the homogeneous pair  $(F, G)$ .

Denote by

$$\mathbb{C}_h[z, t] \times \mathbb{C}_h[z, t] = \{(F, G) \in \mathbb{C}_h[z, t] \times \mathbb{C}_h[z, t] \mid (F, G) \text{ is a homogeneous pair}\}.$$

Given a pair  $R = (F, G) \in \mathbb{C}_h[z, t] \times \mathbb{C}_h[z, t]$ , we have the induced commutative diagram:

$$\begin{array}{ccc} \mathbb{C}^2 & \xrightarrow{R} & \mathbb{C}^2 \\ p \downarrow & & \downarrow p \\ S^{3+} & \xrightarrow{R^S} & S^{3+} \\ q \downarrow & & \downarrow q \\ \mathbf{P}^{1+}(\mathbb{C}) & \xrightarrow{R^P} & \mathbf{P}^{1+}(\mathbb{C}) \end{array}$$

where

$$R((z, t)) = (F((z, t)), G((z, t))) \text{ for } (z, t) \in \mathbb{C}^2, \tag{9}$$

$$R^S((z, t)) = [F((z, t)), G((z, t))] \text{ for } (z, t) \in S^{3+}, \tag{10}$$

$$R^P([z : t]) = [F((z, t)) : G((z, t))] \text{ for } [z : t] \in \mathbf{P}^{1+}(\mathbb{C}). \tag{11}$$

For a prefixed nullity tolerance  $10^{-N}$ , we can define

$$R_N^S = p_N R j, \tag{12}$$

where  $j: S^{3+} \rightarrow \mathbb{C}^2$  is the canonical inclusion, and  $p_N$  is given in (7).

**Remark 2.** We note that many numerical methods are based in the iteration of a rational map  $f(x) = \frac{A(x)}{B(x)}$ . The connection with the methods developed in this work is given by taking  $x = \frac{z}{t}$  and  $F(z, t) = t^d A(\frac{z}{t})$ ,  $G(z, t) = t^d B(\frac{z}{t})$ , where  $d = \text{degree}(f)$ . In this way, we obtain the map  $R = (F, G) : \mathbb{C}^2 \rightarrow \mathbb{C}^2$  which induces the pair of maps  $(R^S, R^P)$ . It is interesting to note that, when  $B(x_0) = 0$ ,  $x_0 = z_0/t_0$ , we have  $G(z_0, t_0) = 0$  and  $R(z_0, t_0) = (F(z_0, t_0), 0) \in \mathbb{C}^2$ .

Since  $R$  is a homogeneous pair of degree  $d$ , one has that  $R^S(\lambda(z, t)) = \lambda^d R^S((z, t))$  if  $|\lambda| = 1$ . Then, there is an induced map  $R_N^P : \mathbf{P}^{1+}(\mathbb{C}) \rightarrow \mathbf{P}^{1+}(\mathbb{C})$ , and we have a commutative diagram:

$$\begin{array}{ccc}
 \mathbb{C}^2 & \xrightarrow{R} & \mathbb{C}^2 \\
 j \uparrow & \nearrow R_j & \downarrow p_N \\
 S^{3+} & \xrightarrow{R_N^S} & S^{3+} \\
 q \downarrow & & \downarrow q \\
 \mathbf{P}^{1+}(\mathbb{C}) & \xrightarrow{R_N^P} & \mathbf{P}^{1+}(\mathbb{C})
 \end{array}$$

where  $R_N^S((z, t)) = [F((z, t)), G((z, t))]_N$  for  $(z, t) \in S^{3+}$  and  $R_N^P([z : t]) = qR_N^S((z, t))$  for  $(z, t) \in S^{3+}$ .

Note that

$$\lim_{N \rightarrow +\infty} R_N^S = R^S, \quad \lim_{N \rightarrow +\infty} R_N^P = R^P. \tag{13}$$

### 3.2. Normalization of a Homogeneous Pair

**Definition 4.** For  $F \in \mathbb{C}_h[z, t]$  given by  $F(z, t) = a_0 t^d + a_1 z t^{d-1} + \dots + a_n z^n t^{d-n}$ , we define the norm  $\|F\|$  by the formula

$$\|F\| = |a_0| + |a_1| + \dots + |a_n|.$$

Suppose that  $(F, G) \in \mathbb{C}_h[z, t] \times \mathbb{C}_h[z, t]$  where  $F(z, t) = a_0 t^d + a_1 z t^{d-1} + \dots + a_n z^n t^{d-n}$  and  $G(z, t) = b_0 t^d + b_1 z t^{d-1} + \dots + b_m z^m t^{d-m}$ . We define the norm of  $(F, G)$  by

$$\|(F, G)\| = \|F\| + \|G\| = |a_0| + |a_1| + \dots + |a_n| + |b_0| + |b_1| + \dots + |b_m|.$$

The normalization  $[F, G]$  of a pair  $(F, G) \in \mathbb{C}_h[z, t] \times \mathbb{C}_h[z, t]$  is given as follows:

$$[F, G] = \begin{cases} (0, 0) & \text{if } (F, G) = (0, 0), \\ (\frac{1}{\|(F, G)\|} F, \frac{1}{\|(F, G)\|} G) & \text{if } (F, G) \neq (0, 0). \end{cases} \tag{14}$$

A homogeneous pair  $(F, G)$  is said to be a normalized pair if  $[F, G] = (F, G)$ .

Denote by  $(\mathbb{C}_h[z, t] \times \mathbb{C}_h[z, t])_{\text{normalized}}$  the subset of normalized homogeneous pairs.

### 3.3. Irreducible Homogeneous Pairs

**Definition 5.** Given  $(F, G) \in \mathbb{C}_h[z, t] \times \mathbb{C}_h[z, t]$ ,  $(F, G)$  is said to be irreducible if either  $(F, G) = (0, 0)$  or  $(F, G) \neq (0, 0)$ , and it satisfies that  $(F, G) = (HF_1, HG_1)$  implies  $\text{degree}(H) = 0$ .

Note that, if  $R = (F, G) \in \mathbb{C}_h[z, t] \times \mathbb{C}_h[z, t]$ , for the map  $R^P = [F : G]$ , the subsets  $\text{Fix}(R^P)$ ,  $\text{PFix}(R^P)$ ,  $\text{Ind}(R^P)$ ,  $\text{PInd}(R^P)$  of  $\mathbf{P}^{1+}(\mathbb{C})$  (see Definition 1) are given by

$$\begin{aligned}
 \text{Fix}(R^P) &= \{[z : t] \mid \text{there exists } \lambda \in \mathbb{C} \setminus \{0\}, F(z, t) = \lambda z, G(z, t) = \lambda t\} \\
 \text{PFix}(R^P) &= \{[z : t] \mid (z, t) \neq (0, 0) \text{ and there exists } \lambda \in \mathbb{C} \setminus \{0\}, F(z, t) = \lambda z, G(z, t) = \lambda t\}
 \end{aligned}$$

$\text{Ind}(R^P) = \{[z : t] | F(z, t) = 0, G(z, t) = 0\}$   
 $\text{PInd}(R^P) = \{[z : t] | (z, t) \neq (0, 0), F(z, t) = 0, G(z, t) = 0\}$ .  
 We also consider the following subsets of  $\mathbf{P}^{1+}(\mathbb{C})$ :

$$\begin{aligned}
 Z(F) &= \{[z : t] | F(z, t) = 0\}, & \text{PZ}(F) &= \{[z : t] | (z, t) \neq (0, 0), F(z, t) = 0\}, \\
 Z(F, G) &= \{[z : t] | F(z, t) = 0, G(z, t) \neq 0\}, & \text{P}(F, G) &= \{[z : t] | F(z, t) \neq 0, G(z, t) = 0\}.
 \end{aligned}$$

**Proposition 1.** *Suppose that  $(F, G) \in \mathbb{C}_h[z, t] \times \mathbb{C}_h[z, t]$  and  $(F, G) \neq (0, 0)$ . Then,*

- (i) *There is  $H_1 \in \mathbb{C}_h[z, t] \setminus \{0\}$  such that  $(F, G) = (H_1F_1, H_1G_1)$  and  $(F_1, G_1) \in \mathbb{C}_h[z, t] \times \mathbb{C}_h[z, t]$  is irreducible.*
- (ii) *If  $(F, G) = (H_1F_1, H_1G_1)$ ,  $(F, G) = (H_2F_2, H_2G_2)$ ,  $H_1, H_2 \in \mathbb{C}_h[z, t] \setminus \{0\}$  and  $(F_1, G_1), (F_2, G_2)$  are irreducible, then  $[F_1 : G_1] = [F_2 : G_2]$ .*
- (iii) *There is  $H \in \mathbb{C}_h[z, t] \setminus \{0\}$  such that  $(F, G) = (HF^{red}, HG^{red})$  and  $(F^{red}, G^{red})$  is a normalized irreducible homogeneous pair.*

**Proof.** (i) and (iii): For any pair  $(F, G) \in \mathbb{C}_h[z, t] \times \mathbb{C}_h[z, t]$ , we have the following particular cases:

If  $F = 0$  and  $G = 0$ , then we take  $F_1 = F^{red} = 0, G_1 = G^{red} = 0$  and, for any  $H_1 \in \mathbb{C}_h[z, t] \setminus \{0\}$ , we have that  $(F, G) = (H_1F_1, H_1G_1)$  and  $(F_1 = F^{red}, G_1 = G^{red})$  is a normalized irreducible pair.

If  $F \neq 0$  and  $G = 0$ , then we take  $F^{red} = 1, G^{red} = 0$  and  $H_1 = F$ . We have that  $(F^{red}, G^{red})$  is a normalized irreducible pair.

If  $F = 0$  and  $G \neq 0$ , then we take  $F_1 = F^{red} = 0, G_1 = G^{red} = 1$  and  $H_1 = G$ . We have that  $(F^{red}, G^{red})$  is a normalized irreducible pair.

Otherwise, we have  $F \neq 0, G \neq 0$  and  $\text{degree}(F) = d = \text{degree}(G)$ : Suppose that  $F(z, t) = t^{e_F}(a_0t^{d-e_F} + a_1zt^{d-1-e_F} + \dots + a_nz^{d-e_F}), G(z, t) = t^{e_G}(b_0t^{d-e_G} + b_1zt^{d-1-e_G} + \dots + b_mz^{d-e_G}), a_n \neq 0$  and  $b_m \neq 0$ .

Take the polynomials  $a(z) = a_0 + a_1z + \dots + a_nz^{d-e_F}, b(z) = b_0 + b_1z + \dots + b_mz^{d-e_G}$  and the canonical factorizations  $a(z) = a_n(z - z_1^p)^{\alpha_1} \dots (z - z_r^p)^{\alpha_r}, b(z) = b_m(z - z_1^q)^{\beta_1} \dots (z - z_s^q)^{\beta_s}$ .

Taking into account the common roots of  $a(z)$  and  $b(z)$  and their multiplicities, we can uniquely take polynomials  $h(z), p_1(z), q_1(z)$  such that  $h(z)$  is monic and  $a(z) = h(z)p_1(z), b(z) = h(z)q_1(z)$ . Note that  $\text{degree}(a(z)) = d - e_F \geq 0, \text{degree}(b(z)) = d - e_G \geq 0$ , then we have  $\text{degree}(h(z)) = d_h \geq 0, \text{degree}(p_1(z)) = d_{p_1} \geq 0$  and  $\text{degree}(q_1(z)) = d_{q_1} \geq 0$ . Taking the operator  $H$  given in (8), we can consider  $K_1 = H(h, d_h), P_1 = H(p_1, d_{p_1}), Q_1 = H(q_1, d_{q_1})$ . Then, one has that  $F = t^{e_F}K_1P_1, G = t^{e_G}K_1Q_1$ . Let  $e = \min\{e_F, e_G\}$  and take  $F_1 = F^{red} = \frac{1}{\|(P_1, Q_1)\|} (t^{e_F-e}P_1), G_1 = G^{red} = \frac{1}{\|(P_1, Q_1)\|} (t^{e_G-e}Q_1), H_1 = \|(P_1, Q_1)\| t^e K_1$ . Then, we have that  $F = H_1F^{red}, G = H_1G^{red}$  and  $(F^{red}, G^{red})$  is a normalized irreducible pair.

(ii): Suppose that  $(F, G) = (H_1F_1, H_1G_1), (F, G) = (H_2F_2, H_2G_2), H_1, H_2 \in \mathbb{C}_h[z, t] \setminus \{0\}$  and  $(F_1, G_1), (F_2, G_2)$  are irreducible. Suppose that  $\text{degree}(F) = \text{degree}(G) > 0$ . Taking into account that  $Z(H_1) = Z(F, G) = Z(H_2)$ , the equations  $F = H_1F_1 = H_2F_2, G = H_1G_1 = H_2G_2$  and that, if  $(z_0, t_0) \in Z(F, G)$ , the multiplicity of  $(z_0, t_0)$  in  $H_1$  is equal to the multiplicity of  $(z_0, t_0)$  in  $H_2$ , it follows that there is  $\alpha \in \mathbb{C} \setminus \{0\}$  such that  $H_2 = \alpha H_1$ . Then,  $H_1F_1 = H_1(\alpha F_2), H_1G_1 = H_1(\alpha G_2)$ . This implies that  $F_1 = \alpha F_2, G_1 = \alpha G_2$ . That is,  $[F_1 : G_1] = [F_2 : G_2]$ . In the other cases, one can also check that  $[F_1 : G_1] = [F_2 : G_2]$ .  $\square$

This gives a canonical reduction process

$$\text{red} : \mathbb{C}_h[z, t] \times \mathbb{C}_h[z, t] \rightarrow (\mathbb{C}_h[z, t] \times \mathbb{C}_h[z, t])_{\text{normalized}}$$

$$R = (F, G) \rightarrow \text{red}(R) = \text{red}((F, G)) = (F^{red}, G^{red}) \tag{15}$$

such that, if  $(F, G) \neq (0, 0)$ , then  $\text{PInd}(\text{red}(R)^P) = \emptyset$ .

Note that, if  $R = (F, G) \in \mathbb{C}_h[z, t] \times \mathbb{C}_h[z, t]$ , and we consider  $R^P = [F : G] \in \text{End}(\mathbf{P}^{1+}(\mathbb{C}))$ ; then, we have:

$$\begin{aligned} \text{Fix}(R^P) &\subset \text{Fix}(\text{red}(R)^P) \subset \text{Fix}(R^P) \cup \text{Ind}(R^P) \\ \text{Ind}(R^P) \setminus \text{Fix}(\text{red}(R)^P) &= \{x \in \mathbf{P}^{1+}(\mathbb{C}) \mid R^P(x) = \bar{0} \text{ and } (\text{red}(R)^P)(x) \neq x\}. \end{aligned}$$

Moreover,  $R = (F, G) \neq (0, 0)$  is irreducible if and only if  $\text{PInd}(R^P) = \emptyset$ .

**Remark 3.** It is interesting to observe that, if  $R = (F, G) \in \mathbb{C}_h[z, t] \times \mathbb{C}_h[z, t]$  is irreducible and  $(F, G) \neq (0, 0)$ , then one has induced maps  $R = (F, G): \mathbb{C}^2 \setminus \{(0, 0)\} \rightarrow \mathbb{C}^2 \setminus \{(0, 0)\}$ ,  $R^S = [F, G]: S^3 \rightarrow S^3$  and  $R^P = [F : G]: \mathbf{P}^1(\mathbb{C}) \rightarrow \mathbf{P}^1(\mathbb{C})$ .

**Remark 4.** Given  $R = (F, G) \in \mathbb{C}_h[z, t] \times \mathbb{C}_h[z, t]$ , one has an induced map of the pointed Hopf fibration:

$$\begin{array}{ccc} S^{3+} & \xrightarrow{R^S=[F,G]} & S^{3+} \\ q \downarrow & & \downarrow q \\ \mathbf{P}^{1+}(\mathbb{C}) & \xrightarrow{R^P=[F:G]} & \mathbf{P}^{1+}(\mathbb{C}) \end{array}$$

and, if  $(F, G) \neq (0, 0)$  is irreducible, we have an endomorphism of the Hopf fibration.

### 3.4. Indeterminacy Search Function of a Homogeneous Pair

In this paper, for a given homogeneous pair  $R = (F, G)$  of degree  $d$ , if  $\mathbb{R}_+ = [0, +\infty)$ , we consider the norm function  $\|\cdot\|: \mathbb{C}^2 \rightarrow \mathbb{R}_+$ ,  $\|(z, t)\| = |z| + |t|$  and the composites

$$\phi = \|\cdot\|R: \mathbb{C}^2 \rightarrow \mathbb{R}_+, \quad \phi^S = \|\cdot\|Rj: S^{3+} \rightarrow \mathbb{R}_+ \tag{16}$$

where  $j: S^{3+} \rightarrow \mathbb{C}^2$  is the canonical inclusion. Note that, if  $|\lambda| = 1$ , then  $\phi^S(\lambda(z, t)) = \|R(\lambda(z, t))\| = \|\lambda^d R((z, t))\| = |\lambda^d| \phi^S((z, t)) = \phi^S((z, t))$ . Therefore, we have an induced map  $\phi^P: \mathbf{P}^{1+}(\mathbb{C}) \rightarrow \mathbb{R}_+$  given by

$$\phi^P([z : t]) = \phi((z, t)) = |F(z, t)| + |G(z, t)|. \tag{17}$$

It is interesting to note that, if  $\text{degree}(R) \neq 0$ , then  $\phi((0, 0)) = \phi^S((0, 0)) = \phi^P(\bar{0}) = 0$ .

**Definition 6.** Given a homogeneous pair  $(F, G)$ , the induced map  $\phi: \mathbb{C}^2 \rightarrow \mathbb{R}_+$  ( $\phi^S: S^{3+} \rightarrow \mathbb{R}_+$ ,  $\phi^P: \mathbf{P}^{1+}(\mathbb{C}) \rightarrow \mathbb{R}_+$ ) is said to be the indeterminacy search function of  $(F, G)$  on  $\mathbb{C}^2$  (respectively on:  $S^{3+}$ ,  $\mathbf{P}^{1+}(\mathbb{C})$ ).

The map  $\phi^P$  has the following properties:

**Theorem 1.** Consider  $\mathbf{P}^{1+}(\mathbb{C})$  as the topological sum of  $\mathbf{P}^1(\mathbb{C})$  and  $\{\bar{0}\}$  and let  $R = (F, G)$  be an homogeneous pair with  $\text{degree}(R) \geq 1$ . Then, for the induced maps  $R^P: \mathbf{P}^{1+}(\mathbb{C}) \rightarrow \mathbf{P}^{1+}(\mathbb{C})$ ,  $\phi^P: \mathbf{P}^{1+}(\mathbb{C}) \rightarrow \mathbb{R}_+$ , we have:

- (i) Given  $[z_0 : t_0] \in \mathbf{P}^{1+}(\mathbb{C})$ ,  $\phi^P([z_0 : t_0]) = 0$  if and only if  $[z_0 : t_0] \in \text{Ind}(R^P)$ .
- (ii)  $[z_0 : t_0] \in \text{Ind}(R^P)$  if and only if for every  $N \in \mathbb{N}$  there is an neighborhood  $U_N$  at  $[z_0 : t_0]$  such that, for every  $[z : t]$  in  $U_N$ ,  $\phi^P([z : t]) \leq 10^{-N}$ .
- (iii)  $[z_0 : t_0] \in \text{Ind}(R^P) \cap \text{Fix}(\text{red}(R)^P)$  if and only if for every  $N \in \mathbb{N}$  and  $C \in \mathbb{N}$  there are neighborhoods  $U_N, U_C$  at  $[z_0 : t_0]$  such that, for every  $[z : t]$  in  $U_N$ ,  $\phi^P([z : t]) \leq 10^{-N}$  and, for every  $[z : t]$  in  $U_C \setminus \{[z_0 : t_0]\}$ ,  $d([z_0 : t_0], R^P([z : t])) \leq 10^{-C}$ .
- (iv) Let  $[z : t]$  be in  $\mathbf{P}^1(\mathbb{C})$  and  $[z_0 : t_0] \in \text{Ind}(R^P) \cap \text{Fix}(\text{red}(R)^P)$ . If  $[z : t]$  is in the basin of  $\text{red}(R)^P$  at  $[z_0 : t_0]$ , then, for every  $N \in \mathbb{N}$  and every  $C \in \mathbb{N}$ , there is  $k_{(N,C)} \in \mathbb{N}$  such that  $\phi^P((R_N^P)^k([z : t])) \leq 10^{-N}$  and  $|\phi^P((R_N^P)^{k-1}([z : t])) - \phi^P((R_N^P)^k([z : t]))| \leq 10^{-C}$  for every  $k \geq k_{(N,C)}$ .

**Proof.** (i): We have that  $\phi^P([z_0 : t_0]) = |F(z_0, t_0)| + |G(z_0, t_0)|$ . Therefore,  $\phi^P([z_0 : t_0]) = 0$  if and only if  $F(z_0, t_0) = 0$  and  $G(z_0, t_0) = 0$ .

(ii): It follows from (i) and the fact that  $\phi^P$  is a continuous map.

(iii): For the case  $[z_0 : t_0] = [0 : 0]$ , we can take  $U_N = U_C = \{[0 : 0]\}$ . Now, we suppose that  $[z_0 : t_0] \in \mathbf{P}^1(\mathbb{C})$ . One implication follows from the continuity properties of functions  $\phi^P$  and  $R^P$  (on  $\mathbf{P}^1(\mathbb{C}) \setminus \text{Ind}(R^P)$ ). Note that  $R^P$  has only a finite number of indeterminate points, then we can suppose that for any  $[z : t]$  in  $U_C \setminus \{[z_0 : t_0]\}$ , we have that  $\text{red}(R)^P([z : t]) = R^P([z : t])$ . We can choose  $[z_C : t_C]$  in  $U_C \setminus \{[z_0 : t_0]\}$  such that  $[z_C : t_C] \rightarrow_{C \rightarrow +\infty} [z_0 : t_0]$ . Then,  $d([z_C : t_C], \text{red}(R)^P([z_C : t_C])) = d([z_C : t_C], R^P([z_C : t_C])) \rightarrow 0$  and  $d([z_C : t_C], \text{red}(R)^P([z_C : t_C])) \rightarrow d([z_0 : t_0], \text{red}(R)^P([z_0 : t_0]))$ . This implies that  $d([z_0 : t_0], \text{red}(R)^P([z_0 : t_0])) = 0$ ; that is,  $[z_0 : t_0] \in \text{Fix}(\text{red}(R)^P)$ . By (ii), we also have that the condition  $\phi^P([z : t]) \leq 10^{-N}$  for all  $[z : t] \in U_C$  implies that  $[z_0 : t_0] \in \text{Ind}(R^P)$ .

(iv): Suppose that  $[z : t]$  be in  $\mathbf{P}^1(\mathbb{C})$ ,  $[z_0 : t_0] \in \text{Ind}(R^P) \cap \text{Fix}(\text{red}(R)^P)$  and  $[z : t]$  is in the basin of  $\text{red}(R)$  at  $[z_0 : t_0]$ . We have that  $\text{red}(R)^P([z_0 : t_0]) = [z_0 : t_0]$ . If  $[z : t]$  is in the basin of  $[z_0 : t_0]$ , given  $C, N \in \mathbb{N}$ , there is  $k_0 \in \mathbb{N}$  such that  $d((\text{red}(R)^P)^k([z : t]), [z_0 : t_0]) \leq \frac{10^{-C}}{2}$  for every  $k \geq k_0$ . Since either  $(R_N^P)^k([z : t]) = (\text{red}(R)^P)^k([z : t])$  or  $(R_N^P)^k([z : t]) = [0 : 0]$  and  $\phi^P$  is continuous and  $\phi^P([z_0 : t_0]) = 0 = \phi^P([0 : 0])$ , there is  $k_1 = k_{(N,C)} \in \mathbb{N}$  such that  $|\phi^P((R_N^P)^{k-1}([z : t])) - \phi^P((R_N^P)^k([z : t]))| \leq 10^{-C}$  and  $\phi^P((R_N^P)^k([z : t])) \leq 10^{-N}$  for every  $k \geq k_{(N,C)}$ .  $\square$

The last property (iv) can be established for  $\phi^S$  as follows:

**Corollary 1.** Consider  $S^{3+}$  as the topological sum of  $S^3$  and  $\{(0,0)\}$  and let  $R = (F, G)$  be a homogeneous pair with  $\text{degree}(R) \geq 1$ . Then, for the induced maps  $R^S : S^{3+} \rightarrow S^{3+}$ ,  $R^P : \mathbf{P}^{1+}(\mathbb{C}) \rightarrow \mathbf{P}^{1+}(\mathbb{C})$ ,  $\phi^S : S^{3+} \rightarrow \mathbb{R}_+$ ,  $\phi^P : \mathbf{P}^{1+}(\mathbb{C}) \rightarrow \mathbb{R}_+$ , we have:

If  $[z : t]$  is in the basin of  $\text{red}(R)^P$  at  $[z_0 : t_0] \in \text{Ind}(R^P) \cap \text{Fix}(\text{red}(R)^P)$ , then, for every  $N \in \mathbb{N}$  and every  $C \in \mathbb{N}$ , there is  $k_{(N,C)} \in \mathbb{N}$  such that

$$\phi^S((R_N^S)^k((z, t))) \leq 10^{-N} \text{ and } |\phi^S((R_N^S)^{k-1}((z, t))) - \phi^S((R_N^S)^k((z, t)))| \leq 10^{-C}$$

for every  $k \geq k_{(N,C)}$ .

Therefore, for a given  $(z, t) \in S^3$ , one can check if, for  $N, C \in \mathbb{N}$ , there is  $k_{(N,C)} \in \mathbb{N}$  satisfying:

Cauchy inequality on  $S^{3+}$ :

$$d((R_N^S)^{k-1}((z, t)), (R_N^S)^k((z, t))) \leq 10^{-C} \text{ for every } k \geq k_{(N,C)}; \tag{18}$$

Cauchy inequality for  $\phi^S$ :

$$|\phi^S((R_N^S)^{k-1}((z, t))) - \phi^S((R_N^S)^k((z, t)))| \leq 10^{-C} \text{ for every } k \geq k_{(N,C)}; \tag{19}$$

Nullity inequality for  $\phi^S$ :

$$\phi^S((R_N^S)^k((z, t))) \leq 10^{-N} \text{ for every } k \geq k_{(N,C)}. \tag{20}$$

These are necessary conditions for  $[z : t]$  to be in the basin of some points  $[z_0 : t_0] \in \text{Ind}(R^P) \cap \text{Fix}(\text{red}(R)^P)$ .

#### 4. Algorithms to Detect the Existence of Proper Indeterminate Points

In the present section, for a given homogeneous pair  $R = (F, G)$ , we develop some algorithms that divide the augmented complex projective line in three disjoint regions (see Tables 1 and 2): the red region Red approaches the proper basin of  $R^P$  at the super-zero point  $[0,0]$ , which is contained in the union of the basins of  $\text{red}(R)^P$  at the end points associated with proper indeterminate points of  $R^P$ , the green region Green is the union

of the proper basins of  $R^P$  at proper fixed points and the black complementary region  $\text{Black} = \mathbf{P}^{1+}(\mathbb{C}) \setminus (\text{Red} \cup \text{Green})$ .

This algorithm is based on the evaluation of the indeterminacy search function  $\phi^S$  associated with a homogeneous pair  $R = (F, G)$  on the orbit of a point on  $S^{3+}$ . The map  $R^S$  (or  $R_N^S$ ) can be iterated for non irreducible pairs  $R = (F, G)$ . Then, it is not necessary to compute previously the lists of indeterminate points of  $R$  or the fixed points of  $\text{red}(R)$ .

We have to take into account that we obtain a graphic approaching the region that is the union of the proper basins at end points of  $R^P$  induced by proper indeterminate points, and we do not know how this region is divided into different proper basins.

#### 4.1. $m$ -Truncated Cauchy Inequality and Nullity Inequality

Let  $R = (F, G)$  be a homogeneous pair with  $\text{degree}(R) \neq 0$  and  $N \in \mathbb{N}$ . Consider the induced maps  $R^S: S^{3+} \rightarrow S^{3+}$ ,  $R_N^S: S^{3+} \rightarrow S^{3+}$ ,  $R^P: \mathbf{P}^{1+}(\mathbb{C}) \rightarrow \mathbf{P}^{1+}(\mathbb{C})$ ,  $R_N^P: \mathbf{P}^{1+}(\mathbb{C}) \rightarrow \mathbf{P}^{1+}(\mathbb{C})$ ,  $\phi^S: S^{3+} \rightarrow \mathbb{R}_+$ ,  $\phi^P: \mathbf{P}^{1+}(\mathbb{C}) \rightarrow \mathbb{R}_+$ . For  $(z, t) \in S^{3+}$ , we are going to work with sequences of the form:

$$((z, t), R_N^S((z, t)), (R_N^S)^2((z, t)), (R_N^S)^3((z, t)), \dots, (R_N^S)^{k-1}((z, t)), (R_N^S)^k((z, t))), \quad (21)$$

$$([z : t], R_N^P([z : t]), (R_N^P)^2([z : t]), (R_N^P)^3([z : t]), \dots, (R_N^P)^{k-1}([z : t]), (R_N^P)^k([z : t])), \quad (22)$$

$$(\phi^S((z, t)), \phi^S(R_N^S((z, t))), \phi^S((R_N^S)^2((z, t))), \dots, \phi^S((R_N^S)^{k-1}((z, t))), \phi^S((R_N^S)^k((z, t)))), \quad (23)$$

$$(\phi^P([z : t]), \phi^P(R_N^P([z : t])), \phi^P((R_N^P)^2([z : t])), \dots, \phi^P((R_N^P)^{k-1}([z : t])), \phi^P((R_N^P)^k([z : t]))). \quad (24)$$

In a computational context, to stop the construction of sequences of the form (21)–(24), we can try to verify if the conditions (18)–(20) are satisfied. However, we have to consider two additional problems: It is not possible to verify this type of condition for every  $k \geq k_{(N,C)}$ , and it is necessary to establish a maximum number of iterations  $m$  of the function  $R_N^S$ .

Therefore, for a given  $(z, t) \in S^3$ , one can check if, for  $N, C \in \mathbb{N}$ , there is  $k_{(N,C,m)} < m$  satisfying the following condition:

$$\begin{aligned} &|\phi^S((R_N^S)^{k_{(N,C,m)}-1}((z, t))) - \phi^S((R_N^S)^{k_{(N,C,m)}}((z, t)))| \leq 10^{-C} \text{ and} \\ &|\phi^S((R_N^S)^{k-1}((z, t))) - \phi^S((R_N^S)^k((z, t)))| > 10^{-C}, \quad 0 < k < k_{(N,C,m)}. \end{aligned} \quad (25)$$

We refer to this condition as the  $m$ -truncated Cauchy inequality for  $\phi^S$ .

For a given  $k \in \mathbb{N}$  such that  $1 \leq k < m$ , we can check if the following condition is satisfied:

$$\text{Nullity inequality: } \phi^S((R_N^S)^k((z, t))) \leq 10^{-N}. \quad (26)$$

We note that the condition (19) implies the existence of  $m \in \mathbb{N}$  such that the condition (25) is verified.

If we have chosen tolerances  $10^{-N}$  and  $10^{-C}$ , we have considered the following algorithm based on the verification of the logical condition (25):

While  $|\phi^S((R_N^S)^{k-1}((z, t))) - \phi^S((R_N^S)^k((z, t)))|$  greater than  $10^{-C}$  and  $k < m$ , then (a) is applied; otherwise, (b) is obtained.

- (a) a new iteration is done and the logical condition is verified again for the new integer  $k + 1$ .
- (b) the output  $(\phi^S((R_N^S)^k((z, t))), k)$  is taken (note that the integer  $k$  depends on the choice of the tolerances  $(N, C)$ ).

For the output of this algorithm, one has two cases:

- If  $k < m$ , then we have that  $k$  verifies condition (25). Since it also depends on  $(z, t)$ , we use the notation  $k = k_{(N,C,m)}((z, t))$ .
- otherwise,  $k = m$ , in this case, condition (25) is not satisfied. The  $k$  in this output will also be denoted by  $k = k_{(N,C,m)}((z, t))$ .

For prefixed tolerances  $N, C$ , a maximum number of iterations  $m$  and the continuous function  $\phi$ , the above algorithm induces the maps:

$$k_{(N,C,m)} : S^3 \rightarrow \mathbb{N}, \tag{27}$$

$$(R_N^S)^{k_{(N,C,m)}} : S^{3+} \rightarrow S^{3+}, \tag{28}$$

$$l(\phi, N, C, m) : \mathbf{P}^1(\mathbb{C}) \rightarrow [0, +\infty), \quad l(\phi, N, C, m)([z : t]) = \phi^S((R_N^S)^{k_{(N,C,m)}((z,t))}((z,t))). \tag{29}$$

In some cases, we reduce notation by writing  $l(\phi) = l(\phi, N, C, m)$ .

It is easy to check that, for a rectangle  $(a, b) \times (c, d)$  which contains the unit disk, the images of the parametrizations  $\alpha : (a, b) \times (c, d) \rightarrow \mathbf{P}^1(\mathbb{C}), (u, v) \rightarrow [u + iv : 1], \beta : (a, b) \times (c, d) \rightarrow \mathbf{P}^1(\mathbb{C}), (u, v) \rightarrow [1 : u + iv]$  cover  $\mathbf{P}^1(\mathbb{C})$  and the two graphics of the maps  $l(\phi)([u + iv : 1])$  and  $l(\phi)([1 : u + iv])$  give a global description of the function  $l(\phi)$ . For example, for the indeterminacy search functions given in Sections 6.1 and 6.2, you can see the graphic of  $l(\phi)$  in the first row of Tables 1 and 2. For these tables, we have taken the rectangle  $(-2.5, 2.5) \times (-2.5, 2.5)$ . In this case,  $\alpha(( -2.5, 2.5) \times (-2.5, 2.5))$  is a “rectangular” neighborhood at “origin point”  $[0 : 1]$  and  $\beta(( -2.5, 2.5) \times (-2.5, 2.5))$  is a “rectangular” neighborhood at the “infinity point”  $[1 : 0]$ .

It is interesting to remark that, as a consequence of the basic properties of  $\phi^P, \phi^S$  given in Theorem 1 and Corollary 1, one has that the restriction of  $l(\phi)$  to the basin of the super-zero point is equal to 0 (modulo some tolerance) and the restriction of  $l(\phi)$  to the basin of a fixed point  $[z_0 : t_0]$  is equal to  $\phi^S((z_0, t_0)) \neq 0$  (modulo some tolerance).

**Remark 5.** In general, if  $k_{(N,C,m)}((z, t)) = m \gg 0$ , the corresponding orbit of  $[z : t]$  does not converge to a fixed point  $[z_0 : t_0]$  (included the super-zero point). However, it is possible that, for some point in the basin of a fixed point  $[z_0 : t_0]$  or in the basin of an indeterminate point, one could have  $k_{(N,C,m)}((z, t)) = m \gg 0$  when the convergence of the orbit of  $[z : t]$  is very slow. In this case, one could run the algorithm again taking a new integer number  $m' \gg m$  to obtain  $k_{(N,C,m')}((z, t)) < m'$ .

If a fixed point  $[z_0 : t_0]$  is very close to a point  $[z_1 : t_1]$  where  $[z_1 : t_1]$  is either a fixed point or an indeterminate point, one can have that  $l(\phi)((z_0, t_0)) < 10^{-N}$ . In this case, these algorithms “can move” points from the basin of a (simple) fixed point to the basin of the super-zero point. One can avoid this situation taking a new  $N' \gg N$ . We note that these algorithms and implementations work modulo tolerances  $10^{-N}$  and  $10^{-C}$ , so when one has a cluster of  $h$  simple roots contained in a very small disk, this type of computational program can take this  $h$ -cluster as a multiple root of order  $h$ . For a study of different methods to analyze this type of cluster, we refer the reader to [17].

**Remark 6.** Let  $(z_0, t_0)$  be the normalized coordinates of a point  $[z_0 : t_0] \in \mathbf{P}^1(\mathbb{C})$ . For prefixed parameters  $(N, C, m)$  and a homogeneous pair  $R = (F, G)$ , we can analyze the function  $k_{(N,C,m)}((z, t))$  when  $[z : t]$  is in a neighborhood  $U$  at  $[z_0 : t_0]$ ; in general, if  $[z_0 : t_0]$  is contained in the basin of a simple fixed point, there is a neighborhood  $U$  at  $[z_0 : t_0]$  in  $\mathbf{P}^1(\mathbb{C})$  such that  $|k_{(N,C,m)}((z, t)) - k_{(N,C,m)}((z_0, t_0))| \leq 1$  for  $[z : t] \in U$ . However, in the basin of the super-zero point, it is easy to find points  $[z_0 : t_0]$  such that the function  $k_{(N,C,m)}((z, t))$  takes many different values  $\leq m$  in a small neighborhood  $U$  at  $[z_0 : t_0]$  (see the third row in Tables 1 and 2).

#### 4.2. Computing Type-Iteration 2-Arrays

Given a pair  $(z, t) \in S^3$  representing a point  $[z : t] \in \mathbf{P}^{1+}(\mathbb{C})$ , using the maps (27)–(29), we can compute

$$(\phi^S((R_N^S)^{k_{(N,C,m)}((z,t))}((z,t))), k_{(N,C,m)}((z,t)))$$

and one has three possibilities:

(a) If  $k_{(N,C,m)}((z, t)) = m$ , then we say that the type  $(z, t)$  is 0 ( $\text{type}((z, t)) = 0$ ). This means that

$$|\phi^S((R_N^S)^{k-1}((z, t))) - \phi^S((R_N^S)^k((z, t)))| > 10^{-C}, \quad 0 < k \leq k_{(N,C,m)}((z, t)).$$

(b) If  $k_{(N,C,m)}((z, t)) < m$  and  $\phi^S((R_N^S)^{k_{(N,C,m)}((z, t))}((z, t))) \leq 10^{-N}$ , then it implies that

$$|\phi^S((R_N^S)^{k-1}((z, t))) - \phi^S((R_N^S)^k((z, t)))| \leq 10^{-C}, \quad 0 < k \leq k_{(N,C,m)}((z, t)).$$

In this case, we say that the type of  $(z, t)$  is 1 ( $\text{type}((z, t)) = 1$ ). This means that the orbit with initial point  $[z : t]$  converges likely to an indeterminate point of  $R^P$ .

(c) If  $k_{(N,C,m)}((z, t)) < m$  and  $\phi^S((R_N^S)^{k_{(N,C,m)}((z, t))}((z, t))) > 10^{-N}$ , then it implies that

$$|\phi^S((R_N^S)^{k-1}((z, t))) - \phi^S((R_N^S)^k((z, t)))| \leq 10^{-C}, \quad 0 < k \leq k_{(N,C,m)}((z, t)).$$

In this case, we say that the type of  $(z, t)$  is 2 ( $\text{type}((z, t)) = 2$ ). That is, the orbit with initial point  $[z : t]$  converges likely to a fixed point of  $R^P$ .

**Remark 7.** Note that, in some exceptional cases, the type of  $(z, t)$  could conduce to misinterpretations. For instance: If for an  $r$ -cycle  $C = (x_0, R^P(x_0), \dots, (R^P)^{r-1}(x_0))$ ,  $x_0 \in \mathbf{P}^1(\mathbb{C})$ , one could have that  $\phi^P(x_0) = \dots = \phi^P((R^P)^{r-1}(x_0)) > 0$ . In this exceptional case, one could have that, if the orbit of a point  $[z : t]$  converges to  $C$ , then  $|\phi^S((R_N^S)^{k_{(N,C,m)}-1}((z, t))) - \phi^S((R_N^S)^{k_{(N,C,m)}}((z, t)))| \leq 10^{-C}$  and  $\phi^S((R_N^S)^{k_{(N,C,m)}}((z, t))) \leq 10^{-N}$ . Then, the algorithm “could move” points from the basin of the  $r$ -cycle  $C$  to the union of the basins of end points induced by proper indeterminate points.

Suppose we have a grid of pairs  $((z, t)_{ij})$  for  $i$  in  $\{1, \dots, u\}$  and, for  $j$  in  $\{1, \dots, v\}$ ,  $u, v \in \mathbb{N}$ ; that is, a 2-array of elements in  $\mathbb{C} \times \mathbb{C}$ . Then, we can compute a 2-array of pairs (type, iteration); that is, a 2-array of elements in  $\{0, 1, 2\} \times \mathbb{N}$  by applying the algorithm above. The existence of points of type 1 is related to the existence of indeterminate points.

One can obtain a graphic representation associated with a homogeneous pair  $R = (F, G)$  using the two parametrizations and the three types  $\{0, 1, 2\}$ . For example, we can choose the black color for type = 0, red color for type = 1, and green color for type = 2. The existence of some regions having a red color, in one of the two rectangles associated with these two parametrizations, means that, for the representation  $R = (F, G)$  of the rational function,  $R^P : \mathbf{P}^{1+}(\mathbb{C}) \rightarrow \mathbf{P}^{1+}(\mathbb{C})$  very likely possesses some indeterminate points.

### 5. Applications to the Relaxed Newton Method

For the relaxed homogeneous Newton method, the existence of indeterminate points is equivalent to the existence of multiple points, and, since non-extraneous fixed points are attracting, tolerances  $10^{-C}$ ,  $10^{-N}$  exist that give a graphic description without ambiguity points.

#### 5.1. The Relaxed Homogeneous Newton Method

Given a polynomial  $p \in \mathbb{C}[x]$ ,  $p(x) = a_0 + a_1x + \dots + a_nx^n$ ,  $a_n \neq 0$ , its derivative polynomial  $p'$  is  $p'(x) = a_1 + 2a_2x + \dots + na_nx^{n-1}$ .

Associating with  $\mu \in \mathbb{C} \setminus \{0\}$ , we consider the homogeneous relaxed Newton method  $\text{HN}_\mu$ :

$$\text{HN}_\mu : \mathbb{C}[x] \rightarrow \mathbb{C}_h[z, t] \times \mathbb{C}_h[z, t]$$

defined by:

$$\text{If } p = 0, \text{HN}_\mu(p) = (0, 0).$$

$$\text{If } p \neq 0, \text{HN}_\mu(p) = (\text{H}(xp' - \mu p, d), \text{H}(p', d)), \text{ where } d = \text{degree}(p) \text{ and } \text{H} : \mathbb{C}[x] \times \mathbb{N} \rightarrow \mathbb{C}_h[z, t] \text{ is the homogenization map defined in Equation (8).}$$

One can also describe the homogeneous relaxed Newton method as follows:

$$\text{HN}_\mu(a_0 + a_1x + \dots + a_nx^n) = (F(z, t), G(z, t)) \tag{30}$$

$$F(z, t) = -\mu a_0 t^n + (a_1 - \mu a_1) z t^{n-1} + \dots + (n a_n - \mu a_n) z^n \tag{31}$$

$$G(z, t) = a_1 t^n + 2 a_2 z t^{n-1} + \dots + n a_n z^{n-1} t \tag{32}$$

where  $(F, G)$  is a homogeneous pair of degree  $n$ .

It is interesting to note that, for  $\mu = 1$ , we obtain the Homogeneous Newton method

$$\text{HN} = \text{HN}_1.$$

With  $p \in \mathbb{C}[x]$  being a polynomial, we can consider the set of roots  $Z(p) = \{x \in \mathbb{C} \mid p(x) = 0\}$ , and the set of multiple roots  $\text{MZ}(p) = \{x \in \mathbb{C} \mid p(x) = 0, p'(x) = 0\}$ .

**Lemma 1.** Let  $b(x) = b_0 + b_1x + \dots + b_mx^m, b_m \neq 0$  be a polynomial. Consider the canonical map  $\alpha: \mathbb{C} \rightarrow \mathbf{P}^1(\mathbb{C}), \alpha(x) = [x : 1]$ . Then,

- (i)  $\alpha|_{Z(b)}: Z(b) \rightarrow Z(H(b, m)) \setminus \{\bar{0}\}$  is a bijection,
- (ii)  $H(xb, m + 1) = zH(b, m), \alpha|_{Z(xb)}: Z(xb) \rightarrow \{[0 : 1]\} \cup (Z(H(b, m)) \setminus \{\bar{0}\})$  is a bijection.
- (iii)  $H(b, m + 1) = tH(b, m), \alpha|_{Z(b)}: Z(b) \rightarrow Z(H(b, m + 1)) \setminus \{\bar{0}, [1 : 0]\}$  is a bijection.

**Proof.** It is a routine check.  $\square$

Now, we can prove the following result:

**Theorem 2.** Let  $p = a_0 + a_1x + \dots + a_nx^n (a_n \neq 0)$  be a polynomial. If  $\mu \neq \text{degree}(p) \geq 1$ , then  $\alpha: \text{MZ}(p) \rightarrow \text{PInd}(\text{HN}_\mu(p)^P), \alpha(x_0) = [x_0 : 1]$ , is a bijection.

**Proof.** Note that

$$H(xp', n)(z, t) = zH(p', n - 1)(z, t).$$

$$\text{HN}_\mu(p)(z, t) = (H(xp', n)(z, t) - \mu H(p, n)(z, t), H(p', n)(z, t)).$$

Suppose  $p(x_0) = 0, p'(x_0) = 0$ . By Lemma 1, we have  $H(p', n - 1)(x_0, 1) = 0, H(p, n)(x_0, 1) = 0$ .

Then,  $H(xp', n)(x_0, 1) - \mu H(p, n)(x_0, 1) = zH(p', n - 1)(x_0, 1) - \mu H(p, n)(x_0, 1) = 0$ . Therefore,  $(\text{HN}_\mu(p))^P([x_0 : 1]) = \bar{0}$ . This implies that  $\alpha(\text{MZ}(p)) \subset \text{PInd}(\text{HN}_\mu(p)^P)$ .

Now, suppose that  $(\text{HN}_\mu(p)^P)([z : t]) = \bar{0}$  and  $[z : t] \neq \bar{0}$ ; that is,  $\text{HN}_\mu(p)(z, t) = (0, 0)$  and  $(z, t) \neq (0, 0)$ . Then,  $H(p', n)(z, t) = 0$ . Note that  $H(p', n)(z, t) = tH(p', n - 1)(z, t)$ . If  $t \neq 0, H(p', n - 1)(z, t) = 0$ . Since  $zH(p', n - 1)(z, t) - \mu H(p, n)(z, t) = 0$ , we have  $H(p, n)(z, t) = 0$ . Therefore, for  $x_0 = z/t$ , we have  $p(x_0) = p'(x_0) = 0$  and  $\alpha(x_0) = [x_0 : 1] = [z : t]$ . If  $t = 0, zH(p', n - 1)(z, 0) - \mu H(p, n)(z, 0) = (n - \mu)a_n z^n \neq 0$ . Then,  $\text{PInd}(\text{HN}_\mu(p)^P) \subset \alpha(\text{MZ}(p))$ .  $\square$

Note that, if  $\mu \neq \text{degree}(p) \in \{0, 1\}$ , then  $\text{MZ}(p) \cong \text{PInd}(\text{HN}_\mu(p)^P) = \emptyset$  and, if  $p = 0$ , then  $\text{MZ}(p) = \mathbb{C}, \text{PInd}(\text{HN}_\mu(p)^P) = \mathbf{P}^1(\mathbb{C})$ .

### 5.2. Graphic Detection of the Existence of Multiple Roots

The algorithm developed in this article to detect the existence of indeterminate points is very interesting when it is applied to the case of the homogeneous Newton and homogeneous relaxed Newton maps.

Let  $p(z)$  be a polynomial of degree  $d \geq 2$ . The standard Newton's method is also called the Newton–Raphson method, and we have that any root of the polynomial  $p(z)$  is a fixed point of the corresponding Newton rational map  $N(p)(z)$  obtained for  $\mu = 1$  in (1). It is well known that a simple root is always super-attractive, and so Newton's method converges quadratically to such roots. At a multiple root of order  $k$ , the eigenvalue

is  $\frac{k-1}{k} < 1$ , and so the method only converges linearly there. The point  $\infty$  is always a repelling fixed point with eigenvalue  $\frac{d}{d-1} > 1$ .

When we take  $N_\mu(p)(z) = \frac{zp'(z) - \mu p(z)}{p'(z)}$ , one has the relaxed Newton’s method. If  $\mu \in \mathbb{N}$ , this relaxed Newton’s method will converge quadratically to a root of order exactly  $\mu$ . We briefly mention the following well-known properties: At a root of order  $k$ , the multiplier of  $N_\mu(p)$  is  $|1 - \frac{\mu}{k}|$ . If  $\mu > 2k$ , then  $|1 - \frac{\mu}{k}| > 1$  and the root will be repelling. If  $\mu < 2k$ , then  $|1 - \frac{\mu}{k}| < 1$  and the convergence will be only linear. If  $\mu = 2k$ , then the root is an indifferent fixed point. The point  $\infty$  is a repelling fixed point with eigenvalue  $\frac{d}{d-\mu}$ .

We have taken into account that, for the Newton method  $N(p)(z) = \frac{zp'(z) - p(z)}{p'(z)}$  and for a root  $z_0$  of the equation  $p(z) = 0$ , one has two cases:

- If  $z_0$  is a simple root, we have that  $N(p)(z_0) = z_0$ ,
- if  $z_0$  is a multiple root, the value of the expression  $N(p)(z) = \frac{zp'(z) - p(z)}{p'(z)}$  at  $z_0$  is not determinate. One could solve this indetermination computing  $\lim_{z \rightarrow z_0} \frac{zp'(z) - p(z)}{p'(z)}$ .

Recall that, in this paper, instead of working with  $N(p)$  or  $N_\mu(p)$ , we consider the homogeneous methods  $HN(p)$  or  $HN_\mu(p)$ , respectively. In these cases, the existence of proper indeterminate points is equivalent to the existence of multiple roots, see Theorem 2. This implies that the algorithm developed in Section 4 can be applied to detect the existence of multiple roots of a polynomial  $p$  using relaxed homogeneous Newton methods.

For the Newton method, taking into account that the roots of a polynomial  $p$  correspond to attractive fixed points of  $\text{red}(HN(p))^P$ , we obtain a graphic representation which gives in red a region approaching the union of proper basins of multiple roots and in green a region approaching the union of proper basins of simple roots. For the relaxed method  $HN_\mu(p)$ , one has a similar graphic result: the red region approaches the union of proper basins of (attractive) multiple roots and the green region approaches the union of proper basins of (attractive) simple roots.

### 6. Examples

In the following subsections, we consider the polynomial  $p(z) = (z^3 - 1)(z - 1)$ , which has  $z = 1$  as a double root and  $z = e^{\frac{2\pi i}{3}}, z = e^{\frac{4\pi i}{3}}$  as simple roots, and we apply the Homogeneous and Homogeneous relaxed Newton methods.

#### 6.1. Graphic Results for the Homogenous Newton Map

Instead of working with the Newton rational map  $N(p)(z) = \frac{-1-2z^3+3z^4}{-1-3z^2+4z^3}$ , our algorithms work with the Homogeneous Newton map:

$$HN(p)(z, t) = (-t^4 - 2z^3t + 3z^4, -t^4 - 3z^2t^2 + 4z^3t).$$

Then, we have the homogeneous bivariate polynomials  $A(z, t) = -t^4 - 2z^3t + 3z^4$  and  $B(z, t) = -t^4 - 3z^2t^2 + 4z^3t$  and the normalized homogeneous pair  $R = (F, G)$ , where  $F(z, t) = \frac{1}{14}(-t^4 - 2z^3t + 3z^4)$  and  $G(z, t) = \frac{1}{14}(-t^4 - 3z^2t^2 + 4z^3t)$ .

Now, we consider the induced map  $\phi: \mathbb{C}^2 \rightarrow [0, +\infty)$  given by

$$\phi((z, t)) = \left| \frac{1}{14}(-t^4 - 2z^3t + 3z^4) \right| + \left| \frac{1}{14}(-t^4 - 3z^2t^2 + 4z^3t) \right|.$$

As we have seen in Section 3.2, we have the induced maps  $\phi^S: S^{3+} \rightarrow [0, +\infty)$ ,  $\phi^P: \mathbb{P}^{1+}(\mathbb{C}) \rightarrow [0, +\infty)$ , and, for prefixed  $N, C, m$ , the map

$$l(\phi, N, C, m): \mathbb{P}^1(\mathbb{C}) \rightarrow [0, +\infty), \quad l(\phi, N, C, m)([z : t]) = \phi^S((R_N^S)^{k(N,C,m)}((z,t))((z,t))),$$

which is briefly denoted by  $l(\phi) = l(\phi, N, C, m)$ .

In the first row of Table 1, using the rectangle  $[-2.5, 2.5] \times [-2.5, 2.5]$ , we have included the graphics of  $l(\phi) = l(\phi, 10, 15, 100)$  on two neighborhoods at  $[0 : 1]$  and at  $[1 : 0]$  by taking the functions  $l(\phi)([\frac{z}{1+|z|} : \frac{1}{1+|z|}])$  and  $l(\phi)([\frac{1}{1+|z|} : \frac{z}{1+|z|}])$ , respectively.

In the second row, we have the red region which approaches the proper basin of the super-zero, and it corresponds to the attraction proper basin of the double root  $z = 1$  of the polynomial  $p(z) = (z^3 - 1)(z - 1) = (z - 1)^2(z - e^{\frac{2\pi i}{3}})(z - e^{\frac{4\pi i}{3}})$ . Note that  $F(\frac{1}{2}, \frac{1}{2}) = \frac{1}{14 \cdot 16}(-1 - 2 + 3) = 0$ ,  $G(\frac{1}{2}, \frac{1}{2}) = \frac{1}{14 \cdot 16}(-1 - 3 + 4) = 0$  and  $\phi((\frac{1}{2}, \frac{1}{2})) = 0$ . Therefore, in this case,  $[1 : 1] = [\frac{1}{2} : \frac{1}{2}]$  is an indeterminate point of  $R = (F, G)$ . Recall that, by Theorem 2,  $MZ(p) \cong PInd(HN(p)^P)$ .

The green region corresponds to points  $z = u + vi$  with  $(u, v) \in [-2.5, 2.5] \times [-2.5, 2.5]$  such that  $k_{(10,15,100)}(\frac{1}{1+|z|}(z, 1)) < 100$  (or  $k_{(10,15,100)}(\frac{1}{1+|z|}(1, z)) < 100$  on the right). This means that, for  $k = k_{(10,15,100)}(\frac{1}{1+|z|}(z, 1))$ :

$$|\phi^S((R_{10}^S)^{k-1}(\frac{1}{1+|z|}(1, z))) - \phi^S((R_{10}^S)^k(\frac{1}{1+|z|}(1, z)))| \leq 10^{-15}$$

and similarly for  $\frac{1}{1+|z|}(1, z)$ . In this case, the green region corresponds to the union of the attraction proper basins associated with the simple roots  $z = e^{\frac{2\pi i}{3}}$  and  $z = e^{\frac{4\pi i}{3}}$ .

In the third row in Table 1, we study the functions  $k_{(10,15,100)}(\frac{1}{1+|z|}(1, z))$  (on the left) and  $k_{(10,15,100)}(\frac{1}{1+|z|}(z, 1))$  (on the right) which take integer values in the interval  $[0, 100]$ . We have associated a different color to each value in  $[0, 100]$ . Now the green region is divided depending on the number of iterations that are necessary to satisfy the 100-truncated Cauchy inequality.

The phenomenon observed in the red region is very interesting. Now the red region appears divided into small pixels having different colors. This means that, for any point  $z_0$  in the red region, the number of iterations  $k_{(10,15,100)}(\frac{1}{1+|z|}(1, z))$  for  $z$  in a neighborhood at  $z_0$  is very unstable; that is, this function takes many different values in this neighborhood.

### 6.2. Graphic Results for the Homogenous Relaxed Newton Map

In this subsection, the relaxation parameter  $\mu$  has been set to  $\mu = 2$ . In this way, we can compare the graphic results obtained for  $\mu = 1$  (Table 1) and for  $\mu = 2$  (Table 2). As in the previous subsection, instead of working with the relaxed Newton rational map  $N_2(p)(z) = \frac{2z^4 - z^3 + z - 2}{4z^3 - 3z^2 - 1}$ , we take the Homogeneous relaxed Newton map:

$$HN_2(p)(z, t) = (-2t^4 + zt^3 - z^3t + 2z^4, -t^4 - 3z^2t^2 + 4z^3t).$$

Then, we have the bivariate polynomials  $A(z, t) = -2t^4 + zt^3 - z^3t + 2z^4$  and  $B(z, t) = -t^4 - 3z^2t^2 + 4z^3t$  and the normalized homogeneous pair  $F(z, t) = \frac{1}{14}(-2t^4 + zt^3 - z^3t + 2z^4)$  and  $G(z, t) = \frac{1}{14}(-t^4 - 3z^2t^2 + 4z^3t)$ .

Now, we consider the induced map  $\phi: \mathbb{C}^2 \rightarrow [0, +\infty)$  given by

$$\phi((z, t)) = |\frac{1}{14}(-2t^4 + zt^3 - z^3t + 2z^4)| + |\frac{1}{14}(-t^4 - 3z^2t^2 + 4z^3t)|.$$

As we have seen in Section 3.2, we have the induced maps  $\phi^S: S^{3+} \rightarrow [0, +\infty)$ ,  $\phi^P: \mathbf{P}^1(\mathbb{C}) \rightarrow [0, +\infty)$ , and, for prefixed  $N, C, m$ , the map

$$l(\phi, N, C, m): \mathbf{P}^1(\mathbb{C}) \rightarrow [0, +\infty), \quad l(\phi, N, C, m)([z : t]) = \phi^S((R_N^S)^{k(N,C,m)((z,t))}((z, t))),$$

and we denote  $l(\phi) = l(\phi, N, C, m)$ .

In the first row of Table 2, using the rectangle  $[-2.5, 2.5] \times [-2.5, 2.5]$ , we have the graphics of  $l(\phi) = l(\phi, 10, 15, 100)$  associated with  $HN_2(p)$  on two neighborhoods at  $[0 : 1]$  and at  $[1 : 0]$ .

In the second row, we have the red region which is the basin of the super-zero, and it corresponds to the attraction basin of the the double root  $z = 1$  of the polynomial  $p(z) = (z^3 - 1)(z - 1) = (z - 1)^2(z - e^{\frac{2\pi i}{3}})(z - e^{\frac{4\pi i}{3}})$ . Note that  $F(\frac{1}{2}, \frac{1}{2}) = \frac{1}{44 \cdot 16}(-2 + 4 - 4 + 2) = 0$ ,  $G(\frac{1}{2}, \frac{1}{2}) = \frac{1}{44 \cdot 16}(-4 + 12 - 12 + 4) = 0$  and  $\phi((\frac{1}{2}, \frac{1}{2})) = 0$ . In this case,  $[1 : 1] = [\frac{1}{2} : \frac{1}{2}]$  is an indeterminate point of  $R = (F, G)$ .

The black region corresponds to points  $z = u + vi$  with  $(u, v) \in [-2.5, 2.5] \times [-2.5, 2.5]$  such that  $k_{(10,15,100)}(\frac{1}{1+|z|}(z, 1)) = 100$  (or  $k_{(10,15,100)}(\frac{1}{1+|z|}(1, z)) = 100$  on the right). This means that

$$|\phi^S((R_{10}^S)^{k-1}(\frac{1}{1+|z|}(1, z))) - \phi^S((R_{10}^S)^k(\frac{1}{1+|z|}(1, z)))| > 10^{-15}, \quad 0 < k \leq 100$$

and similarly for  $\frac{1}{1+|z|}(z, 1)$ .

To compare the Newton method  $HN(p)$  to the relaxed Newton method  $HN_2(p)$ , it is interesting to observe the second rows in Tables 1 and 2. For the  $HN_2(p)$ , the red region in Table 2 is larger than the red region for  $HN(p)$  in Table 1, and the green regions in Table 1 reduce their size and become a black region in Table 2, as we indicated in [6].

In the third row in Table 2, we can see that the functions

$$k_{(10,15,100)}(\frac{1}{1+|z|}(1, z)) \text{ and } k_{(10,15,100)}(\frac{1}{1+|z|}(z, 1))$$

are constant in the black region. Now, the red region appears divided into small pixels having different colors. However, the behavior in Table 2 is different than in Table 1: in some areas (inside of the red region), the function  $k_{(10,15,100)}(\frac{1}{1+|z|}(1, z))$  is stable (locally constant), and, in other areas, it is locally unstable.

### 7. Conclusions

In this work, we have presented a collection of algorithms and implementations based on the representation of a rational map as a self-map of the pointed Hopf fibration  $S^{3+1} \rightarrow \mathbf{P}^{1+}(\mathbb{C})$ . This procedure has the following advantages:

- (i) The use of homogeneous coordinates permits us to work at the point at infinity;
- (ii) The representation of a rational function by a pair of homogeneous bivariate polynomials with the same degree  $R = (F, G)$  allows us to compute the numerical value of the function at any pole point and at the point at infinity;
- (iii) The use of normalized homogeneous coordinates avoids overflow and underflow errors in our algorithms.

One interesting contribution of our algorithms is that the mathematical models  $\mathbf{P}^1(\mathbb{C})$ ,  $S^2$ ,  $S^3$  are improved with the addition of a new element: the super-zero point  $\bar{0}$ . In this way, we get the augmented complex projective line  $\mathbf{P}^{1+}(\mathbb{C}) = \mathbf{P}^1(\mathbb{C}) \cup \{\bar{0} = [0 : 0]\}$  and the corresponding augmented spheres  $S^{2+} = S^2 \cup \{\bar{0} = (0, 0, 0)\}$ ,  $S^{3+} = S^3 \cup \{\bar{0} = (0, 0)\}$ .

- (iv) This permits us to avoid indetermination problems which appear when simultaneously the values of the numerator and denominator of a rational function are equal to zero. In these cases, the super-zero is taken as the image of the indeterminate point.

The study of the proper zeros of the function  $\phi^P : \mathbf{P}^1(\mathbb{C}) \rightarrow \mathbb{R}_+$  helps to study the proper indeterminate points of  $R^P : \mathbf{P}^{1+}(\mathbb{C}) \rightarrow \mathbf{P}^{1+}(\mathbb{C})$ ,  $R^P \neq \bar{0}$ . In general, one considers the associated map  $\text{red}(R)^P$  and, for each point  $x_0 \in \text{PInd}(R^P)$ , we can analyze the corresponding end point induced by  $\text{red}(R)^P : [(x_0, \text{red}(R)^P(x_0), (\text{red}(R)^P)^2(x_0), \dots)]$ . This end point can have different possibilities and properties. For instance, the orbit  $(x_0, \text{red}(R)^P(x_0), (\text{red}(R)^P)^2(x_0), \dots)$  can converge to a fixed point or to a cycle of  $\text{red}(R)^P$ . However, in the particular case that we take the Homogeneous relaxed Newton method  $R = \text{HN}_\mu(p)$ ,  $p \neq 0$ , one has the additional properties  $\text{PFix}(\text{red}(R)^P) = \text{PFix}(R^P) \cup \text{PInd}(R^P)$  and  $\text{PInd}(R^P)$  is bijective with the finite set of multiple roots of the polynomial  $p$ .

- (v) The algorithms developed in this paper and its implementations in Julia language are able to give a graphic approximation to a “red region” which is the union of the attraction basins of multiple roots of a polynomial  $p \neq 0$  when the relaxed Newton method (or the Newton method) is applied. We emphasize the fact that our algorithms do not require the previous calculus of the roots of the corresponding polynomial.
- (vi) The formulation of a homogeneous pair using the maps  $R, R^S, R^P$  in the diagrams

$$\begin{array}{ccc}
 S^{3+} & \xrightarrow{R^S} & S^{3+} \\
 \downarrow & & \downarrow \\
 \mathbf{P}^{1+}(\mathbb{C}) & \xrightarrow{R^P} & \mathbf{P}^{1+}(\mathbb{C})
 \end{array}
 \quad
 \begin{array}{ccc}
 \mathbb{C}^2 & \xrightarrow{R} & \mathbb{C}^2 \\
 \downarrow & & \downarrow \\
 S^{3+} & \xrightarrow{R^S} & S^{3+}
 \end{array}$$

has two advantages: (1) the diagram on the left gives us the relation with analytic maps on the complex projective line, and (2) the diagram on the right permits us to have an easy implementation of our algorithms in Julia language.

- (vii) The implementation in Julia language allows us a fast performance that permits numerical computations and graphic constructions in a short period of time.
- (viii) The techniques developed in this paper can be applied to other families of rational maps—for instance, that obtained with Chebyshev’s method and Halley’s method (note that any iterative method represented by a rational map also admits a homogeneous version).
- (ix) Another interesting line of research appears when we evaluate a continuous map  $\phi: \mathbf{P}^{1+}(\mathbb{C}) \rightarrow [0, +\infty)$  on the orbits of a homogeneous pair (rational map) on  $\mathbf{P}^{1+}(\mathbb{C})$ , so we can compute basins of simple and multiple cycles of a homogeneous pair using Lyapunov functions associated with  $\phi$ .

**Author Contributions:** Investigation, J.I.E.-A., J.M.G.-J., L.J.H.-P. and M.T.R.-R. All authors have contributed equally in this research paper. All authors have read and agreed to the published version of the manuscript.

**Funding:** The research of the first author has been funded by the research group of the University of La Rioja “Geometría, Topología e Historia de las Matemáticas”. The second author has received a grant from the project PGC2018-095896-B-C21 of the Spanish Ministerio de Ciencia, Innovación y Universidades. The third and fourth authors have been funded by the project PID2020-118753GB-I00 of the Spanish Ministerio de Ciencia e Innovación.

**Institutional Review Board Statement:** Not applicable.

**Informed Consent Statement:** Not applicable.

**Data Availability Statement:** Data is contained within the article.

**Conflicts of Interest:** The authors declare no conflict of interest.

## References

1. Varona, J.L. Graphic and numerical comparison between iterative methods. *Math. Intell.* **2002**, *24*, 37–46. [[CrossRef](#)]
2. Amodio, P.; Brugnano, L.; Iavernaro, F.; Mazzia, F. On the use of the Infinity Computer architecture to set up a dynamic precision floating-point arithmetic. *Soft Comput.* **2020**, *24*, 17589–17600. [[CrossRef](#)]
3. Wei, S.; Tang, E.; Liu, T.; Müller, N.T.; Chen, Z. Automatic Numerical Analysis Based on Infinite-Precision Arithmetic. In Proceedings of the 2014 Eighth International Conference on Software Security and Reliability (SERE), San Francisco, CA, USA, 30 June–2 July 2014; pp. 216–224. [[CrossRef](#)]
4. García-Calines, J.M.; Gutiérrez, J.M.; Hernández, L.J.; Rivas, M.T. Graphical representations for the homogeneous bivariate Newton’s method. *Appl. Math. Comput.* **2015**, *269*, 988–1006. [[CrossRef](#)]
5. Gutiérrez, J.M.; Hernández, L.J.; Marañón, M.; Rivas, M.T. Influence of the multiplicity of the roots on the basins of attraction of Newton’s method. *Numer. Algorithms* **2014**, *66*, 431–455. [[CrossRef](#)]
6. Gutiérrez, J.M.; Hernández, L.J.; Magreñán, Á.A.; Rivas, M.T. Measures of the basins of attracting n-cycles for the relaxed Newton’s method. In *Advances in Iterative Methods for Nonlinear Equations*; Plata, S.A., Sáez, S.B., Eds.; Springer: Berlin/Heidelberg, Germany, 2016; pp. 211–246.

7. Hopf, H. Über die Abbildungen der dreidimensionalen Sphäre auf die Kugelfläche. In *Mathematische Annalen*; Springer: Berlin, Germany, 1931; Volume 104, pp. 637–665. [[CrossRef](#)]
8. Gilbert, W.J. The complex dynamics of Newton's method for a double root. *Comput. Math. Applic.* **1991**, *22*, 115–119. [[CrossRef](#)]
9. Vázquez-Lozano, J.E.; Cordero, A.; Torregrosa, J.R. Dynamical analysis on cubic polynomials of damped Traub's method for approximating multiple roots. *Appl. Math. Comput.* **2018**, *328*, 82–99. [[CrossRef](#)]
10. Yang, W. Symmetries of the Julia sets of Newton's method for multiple roots. *Appl. Math. Comput.* **2010**, *217*, 2490–2494. [[CrossRef](#)]
11. Argyros, I.K.; Gutiérrez, J.M.; Magreñán, Á.A.; Romero, N. Convergence of the relaxed Newton's method. *J. Korean Math. Soc.* **2014**, *51*, 137–162. [[CrossRef](#)]
12. von Haeseler, F.; Kriete, H. The relaxed Newton's method for rational functions. *Random Comput. Dynam.* **1995**, *3*, 71–92.
13. Hernández, L.J. Bivariate Newton-Raphson method and toroidal attraction basins. *Numer. Algorithms* **2016**, *71*, 349–381. [[CrossRef](#)]
14. Hernández, L.J.; Marañón, M.; Rivas, M.T. Plotting basins of end points of rational maps with Sage. *Tbilisi Math. J.* **2012**, *5*, 71–99.
15. Extremiana, J.I.; Gutiérrez, J.M.; Hernández, L.J.; Rivas, M.T. An implementation in Julia language for the iteration of rational functions on the Riemann sphere. *Appl. Numer. Methods* **2019**. [[CrossRef](#)]
16. Bezanson, J.; Edelman, A.; Karpinski, S.; Shah, V.B. Julia: A Fresh Approach to Numerical Computing. *SIAM Rev.* **2017**, *59*, 65–98. [[CrossRef](#)]
17. Rump, S.M. Ten methods to bound multiple roots of polynomials. *J. Comput. Appl. Math.* **2003**, *156*, 403–432. [[CrossRef](#)]
18. Beardon, A.F. *Iteration of Rational Functions*; Graduate Texts in Mathematics; Springer: New York, NY, USA, 1991.
19. Milnor, J.W. Dynamics in one complex variable: Introductory lectures. *arXiv* **1990**, arXiv:math/9201272
20. Sullivan, D. Conformal dynamical systems. In *Geometric Dynamics. Lecture Notes in Mathematics*; Palis, J., Ed.; Springer: Berlin/Heidelberg, Germany, 1983; Volume 1007.